

1 **Detail response to the Reviewer comments, BG-2019-291**

2  
3 We thank the reviewer for the comments and for identifying some remaining issues.  
4 Below we provide a point by point response essentially adopting all comments and  
5 suggestions. We hope make the paper ready for publication.

6  
7  
8 The quality of manuscript is significantly improved by authors, and is now close to the  
9 publication in the journal.

10  
11 **Response:** Thank you.

12  
13  
14 Before the accept, I feel there is a little bit more of needs of revision and/or re-  
15 consideration for some specific points in the manuscript. Some of them are very  
16 confusing for readers to understand the manuscript easily.

17  
18  
19 Those specific points are as follow:  
20 L13: “measured” should be “were”

21  
22 **Response:** Corrected.

23  
24  
25 L121: “An instrumented eddy covariance tower” should be “An instrumented eddy  
26 covariance (EC) tower”

27  
28 **Response:** Corrected.

29  
30  
31 L224: In order to secure reliability of the Keeling plot approach in the present study site,  
32 add a sentence, which is similar to the sentence in L166-L167 of Author’s response (i.e.  
33 “We must conclude of course that....”), after the sentence ended with “....to avoid this  
34 caveat”.

35  
36 **Response:** We added the sentence as suggested.

37  
38  
39 L256: “The analytical precision was 0.1%” should be “The analytical precision was  
40 0.1‰”?

41  
42 **Response:** Corrected.

43  
44  
45 L269: “The precision was 0.1%” should be “The precision was 0.1‰”?

46  
47 **Response:** Corrected.

48  
49  
50 L271-L286: Because “RI” in Eq.12 is very confusing with “RI” in Table 3 (RI means  
51 foliage respiration here), “RI” in Eq.12 should be “ALP” or something else which makes  
52 it to be easier to imagine the aboveground litter production.  
53  
54 **Response:** As suggested, we replaced the RI with  $R_{alp}$  for the aboveground litter  
55 production.  
56  
57  
58 L305: “ $r = 0.62$ ” should be “ $r = -0.62$ ”.  
59  
60 **Response:** Corrected.  
61  
62  
63 L306: “ $r = 0.45$ ” should be “ $r = -0.45$ ”.  
64  
65 **Response:** Corrected.  
66  
67  
68 L337: The sentence “daily  $R_s$  values could reach  $6.1 \mu\text{mol m}^{-2} \text{s}^{-1}$ ” is true? There is no  
69  $R_s$  data over the value of  $5 \mu\text{mol m}^{-2} \text{s}^{-1}$  in Figure S1-6 nor Figure 2.  
70  
71 **Response:** Checked and this value is correct but refers to the under trees (UT)  
72 microsite while Fig. 2 shows integrated mean values. To clarify the sentence we added  
73 “**i.e. in the UT microsite; data not shown**”.  
74  
75  
76 L340: Delete “(Fig. S1-6)”.  
77  
78 **Response:** Corrected. It refers to SI Fig. 6.  
79  
80  
81 L349: Add “(no data in any of figures nor tables)” after “( $r = 0.2$  and  $348 \pm 0.1$ ,  
82 respectively;  $p < 0.01$ )”.  
83  
84 **Response:** We added the sentence.  
85  
86  
87 L351: Add “(no data in any of figures nor tables)” after “(CV~40%)”.  
88  
89 **Response:** Added as suggested: “**(correlations and CV values were not included in**  
90 **figures and tables)**”.  
91  
92  
93 L359: “Refluxes” should be “Re fluxes”.  
94  
95 **Response:** Corrected.

96  
97  
98  
99  
100  
101  
102  
103  
104  
105  
106  
107  
108  
109  
110  
111  
112  
113  
114  
115  
116  
117  
118  
119  
120  
121  
122  
123  
124  
125  
126  
127  
128  
129  
130  
131  
132  
133  
134  
135  
136  
137  
138  
139  
140  
141  
142  
143

L373: “being highest” should be “being the highest”.

**Response:** Corrected.

L377: “Repartitioning” should be “Re partitioning”.

**Response:** Corrected.

L382: Add “(Fig. 2)” after “limited water loss”.

**Response:** We added the (Fig. 2).

L409: What does “Despite relatively high rates of respiration fluxes” mean? According to Table 3, the magnitude of Re is only 75% of GPP. Add clear description for “relatively high rates of respiration fluxes”.

**Response:** Thank you. The sentence was revised for clarity.  
**“These rates of respiration fluxes translated at the ecosystem scale to Re/GPP of ~75%, lower than observed in other ecosystems (SI Table 3) and leading, in turn, to high ecosystem CUE of 0.43”**

L417-L418: “presented n Table 3” should be “presented in Table 3”.

**Response:** Corrected.

L418-L419: “the belowground allocation” should be “the TBCA”.

**Response:** Corrected.

L419-L423: This sentence is very confusing. Does this sentence mean that “While there is little change in the ratio of the respiration components to Re or to GPP, the shift from the autotrophic components (i.e. Rsa, RI, and Rw) to the heterotrophic component (i.e. Rh) has occurred as indicated by increasing ratio of Rh to Rsa + RI + Rw from 0.27 in 2003 to 0.37 in 2015.” ?

**Response:** We revised this sentence for clarity.

L467: “the remarkable increase” may be prefer than “the marked increase”.

144 **Response:** Wording changed.

145

146

147 L468-L472: This sentence would be better to be changed as “Here, because comparing  
148 the non-continuous data from the present (2016) and earlier (2001–2006) studies is  
149 sensitive to the large interannual variations in the ecosystem activities and fluxes  
150 (Qubaja et al., in press), we focused on the more robust changes in the ratio of the  
151 respiration components to the overall fluxes (Re) (Table 3)”.

152

153 **Response:** Wording changed as suggested.

154

155

156 Figure 3: Caption should be “a) The seasonal variations in the relative contribution of  
157 soil autotrophic (Rsa), heterotrophic (Rh), and abiotic (Ri) components to Rs, and b)  
158 seasonal variations in the relative contribution of soil autotrophic (Rsa), heterotrophic  
159 (Rh), abiotic (Ri), and foliage and stem respiration (Rf is obtained from the Re-Rs)  
160 components to ecosystem respiration (Re) during eight campaigns (Jan–Sep) in 2016.  
161 The contributions were determined with linear mixing models using isotope signature  
162 analysis ( $\delta^{13}\text{C}$  and  $\Delta^{14}\text{C}$ ) of soil CO<sub>2</sub> profile from 0 to 120 cm soil depth. These  
163 results confirmed earlier estimates of Grünzweig et al. (2009) and Maseyk et al.  
164 (2008a)”.

165

166 **Response:** The caption was re-arranged as suggested.

167

168

169 Figures 2, 3, SI-6: Please consider to add vertical lines representing the periods of  
170 spring, summer, autumn, and winters. In the manuscript, seasonal characteristic of  
171 fluxes is one of the mainly focused topics; however, it is difficult to identify those from  
172 figures without the visually representing period of individual season.

173

174 **Response:** We added the vertical lines as suggested and indicate it in the captions

175

176

177 Finally, please run careful refining of every sentences in the manuscript again, in order  
178 to avoid unnecessary confusion.

179

180 **Response:** Done

181 **Partitioning of canopy and soil CO<sub>2</sub> fluxes in a pine forest at the dry**  
182 **timberline across a 13-year observation period**

183 **Rafat Qubaja<sup>a</sup>, Fyodor Tatarinov<sup>a</sup>, Eyal Rotenberg<sup>a</sup>, and Dan Yakir<sup>a\*</sup>**

184 <sup>a</sup> Department of Earth and Planetary Sciences, Weizmann Institute of Science, Rehovot 76100, Israel

185 \*Correspondence: Dan Yakir; email: [dan.yakir@weizmann.ac.il](mailto:dan.yakir@weizmann.ac.il)

186 **Abstract**

187 Partitioning carbon fluxes is key to understanding the process underlying ecosystem response to change.  
188 This study used soil and canopy fluxes with stable isotopes (<sup>13</sup>C) and radiocarbon (<sup>14</sup>C) measurements in  
189 an 18 km<sup>2</sup>, 50-year-old dry (287 mm mean annual precipitation; non-irrigated) *Pinus halepensis* forest  
190 plantation in Israel to partition the net ecosystem's CO<sub>2</sub> flux into gross primary productivity (GPP) and  
191 ecosystem respiration (Re) and (with the aid of isotopic measurements) soil respiration flux (Rs) into  
192 autotrophic (Rsa), heterotrophic (Rh), and inorganic (Ri) components. On an annual scale, GPP and Re  
193 ~~measured were~~ 655 and 488 g C m<sup>-2</sup>, respectively, with a net primary productivity (NPP) of 282 g C m<sup>-2</sup>  
194 and carbon-use efficiency (CUE=NPP/GPP) of 0.43. Rs made up 60% of the Re and comprised 24 ± 4%,  
195 23 ± 4%, and 13 ± 1% from Rsa, Rh, and Ri, respectively. The contribution of root and microbial respiration  
196 to Re increased during high productivity periods, and inorganic sources were more significant components  
197 when the soil water content was low. Comparing the ratio of the respiration components to Re of our mean  
198 2016 values to those of 2003 (mean for 2001–2006) at the same site indicated a decrease in the autotrophic  
199 components (roots, foliage, and wood) by about -13%, and an increase in the heterotrophic component  
200 (Rh/Re) by about +18%, with similar trends for soil respiration (Rsa/Rs decreasing by -19% and Rh/Rs  
201 increasing by +8%, respectively). The soil respiration sensitivity to temperature (Q<sub>10</sub>) decreased across the  
202 same observation period by 36% and 9% in the wet and dry periods, respectively. Low rates of soil carbon  
203 loss combined with relatively high belowground carbon allocation (i.e., 38% of canopy CO<sub>2</sub> uptake) and  
204 low sensitivity to temperature help explain the high soil organic carbon accumulation and the relatively  
205 high ecosystem CUE of the dry forest.

206  
207 **Keywords:** Carbon balance, Soil respiration, Autotrophic, Heterotrophic, Inorganic flux, Temperature  
208 response, Semi-arid ecosystem, Pine forest, Canopy cover, Soil chamber

## 209 1. Introduction

210 The annual net storage of carbon in the land biosphere, known as net ecosystem production (NEP), is the  
211 balance between carbon uptake during gross primary productivity (GPP) and carbon loss during growth,  
212 maintenance respiration by plants (i.e., autotrophic respiration,  $R_a$ ), and decomposition of litter and soil  
213 organic matter (i.e., heterotrophic respiration,  $R_h$ ; Bonan, 2008). The difference between GPP and  $R_a$   
214 expresses the net primary production (NPP) and is the net carbon uptake by plants that can be used for new  
215 biomass production. Measurements from a range of ecosystems have shown that total plant respiration can  
216 be as large as 50% of GPP (e.g., Etzold et al., 2011) and together with  $R_h$  comprises total ecosystem  
217 respiration ( $R_e$ ,  $R_e=R_a+R_h$ ). The partitioning of the ecosystem carbon fluxes can therefore be summarized  
218 as:

$$219 \quad GPP = NPP + R_a = NEP + R_h + R_a \quad (1)$$

220 Earlier campaign-based measurements carried out by Maseyk et al. (2008a) and Grünzweig et al. (2009)  
221 in the semi-arid *Pinus halepensis* (Aleppo pine) Yatir forest indicated that GPP at this site was lower than  
222 among temperate coniferous forests (1,000–1,900 g C m<sup>-2</sup> y<sup>-1</sup>) but within the range estimated for  
223 Mediterranean evergreen needle-leaf and boreal coniferous forests (Falge et al., 2002; Flechard et al.,  
224 2019b), and had a high carbon-use efficiency of 0.4 (CUE = NPP/GPP; DeLucia et al., 2007). The total  
225 flux of CO<sub>2</sub> released from the ecosystem ( $R_e$ ) can be partitioned into aboveground autotrophic respiration  
226 (i.e., foliage and sapwood,  $R_f$ ) and soil CO<sub>2</sub> flux ( $R_s$ ).  $R_s$ , in turn, is a combination of three principal  
227 components and can be further partitioned into the components originating from roots or rhizospheres and  
228 mycorrhizas (i.e., belowground autotrophic,  $R_{sa}$ ), from carbon respired during the decomposition of dead  
229 organic matter by soil microorganisms and macrofaunal (heterotrophic respiration,  $R_h$ ; Bahn et al., 2010;  
230 Kuzyakov, 2006), and pedogenic or anthropogenic acidification of soils containing CaCO<sub>3</sub> ( $R_i$ ; Joseph et  
231 al., 2019; Kuzyakov, 2006), which is expressed as:

$$232 \quad R_e = R_s + R_f = [R_{sa} + R_h + R_i] + R_f \quad (2)$$

233 Previously published results show that the contribution of  $R_{sa}$  and  $R_h$  to  $R_s$  ranges from 24 to 65% and  
234 from 29 to 74%, respectively, in forest soils in different biomes and ecosystems (Binkley et al., 2006; Chen  
235 et al., 2010; Flechard et al., 2019a; Frey et al., 2006; Hogberg et al., 2009; Subke et al., 2011). Some studies  
236 reported significant proportions of abiotic contribution to  $R_s$ , ranging between 10 and 60% (Martí-Roura  
237 et al., 2019; Ramnarine et al., 2012; Joseph et al., 2019). However, most of these experiments were  
238 performed in boreal, temperate, or subtropical forests, and there is a general lack of information on water-  
239 limited environments, such as dry Mediterranean ecosystems. Using both <sup>13</sup>C and CO<sub>2</sub>/O<sub>2</sub> ratios also  
240 showed that abiotic processes, such as CO<sub>2</sub> storage, transport, and interactions with sediments, can  
241 influence  $R_s$  measurements at such sites (Angert et al., 2015; Carmi et al., 2013). Furthermore, root-

242 respired CO<sub>2</sub> can also be dissolved in the xylem water and carried upward with the transpiration stream  
243 (Etzold et al., 2013).

244 Rates of the soil-atmosphere CO<sub>2</sub> flux (Rs) have been altered owing to global climatic change, particularly  
245 through changes in soil temperature (Ts) and soil moisture (SWC; Bond-Lamberty and Thomson, 2010;  
246 Buchmann, 2000; Carvalhais et al., 2014; Hagedorn et al., 2016; Zhou et al., 2009), which could account  
247 for 65–92% of the variability of Rs in a mixed deciduous forest (Peterjohn et al., 1994). Soil moisture  
248 impacts on Rs have been observed in arid and Mediterranean ecosystems, where Ts and SWC are  
249 negatively correlated (e.g., Grünzweig et al., 2009). CO<sub>2</sub> efflux generally increases with increasing soil  
250 temperatures (Frank et al., 2002), which can produce positive feedback on climate warming (Conant et al.,  
251 1998), converting the biosphere from a net carbon sink to a carbon source (IPCC-AR5 2014). A range of  
252 empirical models have been developed to relate Rs rate and temperature (Balogh et al., 2011; Lellei-Kovács  
253 et al., 2011), and the most widely used models rely on the Q<sub>10</sub> approach (Bond-Lamberty and Thomson,  
254 2010), which quantifies the sensitivity of Rs to temperature and can integrate it with physical processes,  
255 such as the rate of O<sub>2</sub> diffusion into and CO<sub>2</sub> diffusion out of soils and the intrinsic temperature dependency  
256 of enzymatic processes (Davidson and Janssens, 2006). Soil moisture (SWC) may be of greater importance  
257 than temperature in influencing Rs in water-limited ecosystems (Hagedorn et al., 2016; Grünzweig et al.,  
258 2009; Shen et al., 2008). In general, the Rs rate increases with the increase of SWC at low levels but  
259 decreases at high levels of SWC (Deng et al., 2012; Hui and Luo, 2004; Jiang et al., 2013). Several studies  
260 highlight the sensitivity of carbon fluxes in semi-arid Mediterranean ecosystems to the irregular seasonal  
261 and interannual distribution of rain events (Poulter et al., 2014; Ross et al., 2012). While Rs is generally  
262 constrained by low SWC during summer months, abrupt and large soil CO<sub>2</sub> pulses have been observed  
263 after rewetting the dry soil (Matteucci et al., 2015).

264 The objectives were twofold. First, to obtain detail on partitioning of the carbon fluxes in a semi-arid pine  
265 forest to help explain the high productivity and carbon use efficiency recently reported for this ecosystem  
266 (Qubaja et al., in press), and provide process-based information to assess the carbon sequestration potential  
267 of such a semi-arid afforestation system. Second, to combine this 2016 study with the results of a similar  
268 one at the same site in 2003 (mean values for 2001–2006; Grünzweig et al., 2007, 2009) to obtain a long-  
269 term perspective across 13 years on soil respiration and its partitioning. We hypothesized that the high  
270 carbon use efficiency of the dry forest ecosystem is associated with high belowground carbon allocation  
271 and relatively low decomposition rates, and that the long-term trend associated with warming may be  
272 suppressed by the dry conditions.

## 273 **2. Materials and methods**

## 274 2.1. Site description

275 The Yatir forest (31°20'49" N; 35°03'07" E, 650 m a.s.l.) is situated in the transition zone between sub-  
276 humid and arid Mediterranean climates (SI Fig. 1) on the edge of the Hebron mountain ridge. The  
277 ecosystem is a semi-arid pine afforestation established in the 1960s and covering approximately 18 km<sup>2</sup>.  
278 The average air temperatures for January and July are 10.0 °C and 25.8 °C, respectively. Mean annual  
279 potential evapotranspiration (ET) is 1,600 mm, and mean annual precipitation is 287 mm. Only winter  
280 (December to March) precipitation occurs in this region, creating a distinctive wet season, while summer  
281 (June to October) is an extended dry season. There are short transition periods between seasons, with a  
282 wetting season (i.e., autumn) and a drying season (i.e., spring). The forest is dominated by Aleppo pine  
283 (*Pinus halepensis* Mill.), with smaller proportions of other pine species and cypress and little understory  
284 vegetation. Tree density in 2007 was 300 trees ha<sup>-1</sup>; mean tree height was 10.0 m; diameter at breast height  
285 (DBH) was ~15.9 cm; and the leaf area index (LAI) was ~1.5. The native background vegetation was  
286 sparse shrubland, which is dominated by the dwarf shrub *Sarcopoterium spinosum* (L.) Spach, with patches  
287 of herbaceous annuals and perennials reaching a total vegetation height of 0.30–0.50 m (Grünzweig et al.,  
288 2003, 2007). The root density range is 30–80 roots m<sup>-2</sup> at the upper 0.1 m soil depth, falling to the minimum  
289 value (~0 roots m<sup>-2</sup>) at 0.7 m soil depth (Preisler et al., 2019). Biological soil crust (BSC) is evident in the  
290 forest but is less than in the surrounding shrub by ~40% (Gelfand et al., 2012).

291 The soil at the research site is shallow (20–40 cm), reaching only 0.7–1.0 m; the stoniness fraction for the  
292 soil depth (0–1.2 m) is 15–60%, and the rock cover of the surface ranges between 9 and 37%, as recently  
293 described in detail (Preisler et al., 2019); the soil is eolian-origin loess with a clay-loam texture (31% sand,  
294 41% silt, and 28% clay; density:  $1.65 \pm 0.14$  g cm<sup>-3</sup>) overlying chalk and limestone bedrock. Deeper soils  
295 (up to 1.5 m) are sporadically located at topographic hollows. While the natural rocky hill slopes in the  
296 region are known to create flash floods, the forested plantation reduces runoff dramatically to less than 5%  
297 of annual rainfall (Shachnovich et al., 2008). Groundwater is deep (>300 m), reducing the possibility of  
298 groundwater recharge due to negative hydraulic conductivity or of water uptake by trees from the  
299 groundwater.

## 300 2.2. Flux and meteorological measurements

301 An instrumented eddy covariance [\(EC\)](#) tower was erected in the geographical center of Yatir forest,  
302 following the EUROFLUX methodology (Aubinet et al., 2000). The system uses a three-dimensional (3D)  
303 sonic anemometer (Omnidirectional R3, Gill Instruments, Lymington, UK) and a closed path LI-COR  
304 7000 CO<sub>2</sub>/H<sub>2</sub>O gas analyzer (LI-COR Inc., Lincoln, NE, USA) to measure the evapotranspiration flux (ET)  
305 and net CO<sub>2</sub> flux (NEE). EC flux measurements were used to estimate the annual scale of NEP by



306 integrating half-hour NEE values. The long-term operation of our EC measurement site (since 2000; see  
 307 Rotenberg and Yakir, 2010) provides continuous flux and meteorological data with about 80% coverage,  
 308 which are subjected to  $U^*$  night-time correction and quality control, and gap filling is based on the extent  
 309 of the missing data, as recently described in more detail in Tatarinov et al. (2016). A site-specific algorithm  
 310 was used for flux partitioning into  $R_e$  and GPP. Daytime ecosystem respiration ( $R_{e-d}$ , in  $\mu\text{mol m}^{-2} \text{s}^{-1}$ ) was  
 311 estimated based on measured night-time values ( $R_{e-n}$ ; i.e., when the global radiation was  $<5 \text{ W m}^{-2}$ ),  
 312 averaged for the first three half-hours of each night. The daytime respiration for each half-hour was  
 313 calculated according to Eq. 3 (Maseyk et al., 2008a; Tatarinov et al., 2016):

$$314 \quad R_{e-d} = R_{e-n}(\alpha_1\beta_s^{dT_s} + \alpha_2\beta_w^{dT_a} + \alpha_3\beta_f^{dT_a}) \quad (3)$$

315 where  $\beta_s$ ,  $\beta_w$ , and  $\beta_f$  are coefficients that correspond to soil, wood, and foliage, respectively;  $dT_s$  and  $dT_a$   
 316 are soil and air temperature deviations from the values at the beginning of the night; and  $\alpha_1$ ,  $\alpha_2$ , and  $\alpha_3$  are  
 317 partitioning coefficients fixed at 0.5, 0.1, and 0.4, respectively. The  $\beta_s$ ,  $\beta_w$ , and  $\beta_f$  coefficients were  
 318 calculated as follows:  $\beta_s$  values were based on  $Q_{10}$  from the Grünzweig et al. (2009) study at the same site;  
 319 where  $\beta_s = 2.45$  for wet soil (i.e., SWC in the upper 30 cm above 20% vol);  $\beta_s = 1.18$  for dry soil (i.e.,  
 320 SWC in the upper 30 cm equal to or below 20% vol);  $\beta_f = 3.15 - 0.036 T_a$ ; and  $\beta_w = 1.34 + 0.46 \exp(-$   
 321  $0.5((\text{DoY}-162)/66.1)^2)$ , where DoY is the day of the hydrological year starting from 1 October. Finally,  
 322 GPP was calculated as  $\text{GPP} = \text{NEE} - R_e$ . Negative values of the NEE and GPP indicated that the ecosystem  
 323 was a  $\text{CO}_2$  sink.

324 Half-hour auxiliary measurements used in this study included photosynthetic activity radiation (PAR mol  
 325  $\text{m}^{-2} \text{s}^{-1}$ ), vapor pressure deficit (VPD, kPa), wind speed ( $\text{m s}^{-1}$ ), and relative humidity (RH, %), with  
 326 additional measurements as described elsewhere (Tatarinov et al., 2016). Furthermore, the soil  
 327 microclimatology half-hour measurements were measured and calculated with soil chamber  
 328 measurements, using the LI-8150-203 (LI-COR, Lincoln, NE), as described below, namely air temperature  
 329 ( $T_a$ ,  $^{\circ}\text{C}$ ) and relative humidity (RH, %) at 20 cm above the soil surface and soil temperature ( $T_s$ ,  $^{\circ}\text{C}$ ) at a  
 330 5 cm soil depth using a soil temperature probe, as well as volumetric soil water content ( $\text{SWC}_{0-10}$ ,  $\text{m}^3 \text{m}^{-3}$ )  
 331 in the upper 10 cm of the soil near the chambers, using the ThetaProbe model ML2x (Delta-T Devices  
 332 Ltd., Cambridge, UK), which was calibrated to the soil composition based on the manufacturer's equations.

### 333 **2.3. Soil $\text{CO}_2$ fluxes**

334 Soil  $\text{CO}_2$  fluxes ( $R_s$ ) were measured with automated non-steady-state systems, using 20 cm diameter  
 335 opaque chambers and a multiplexer to allow for simultaneous control of several chambers (LI -8150, -  
 336 8100-101, -8100-104; LI-COR, Lincoln, NE). The precision of  $\text{CO}_2$  measurements in the chambers' air is  
 337  $\pm 1.5\%$  of the measurements' range (0–20,000 ppm). The chambers were closed on preinstalled PVC collars

338 20 cm diameter, allowing for short measurement time (i.e., 2 min), and positioned away from the collars  
 339 for the rest of the time. Data were collected using a system in which air from the chambers was circulated  
 340 (2.5 l min<sup>-1</sup>) through an infrared gas analyzer (IRGA) to record CO<sub>2</sub> (μmol CO<sub>2</sub>/mol air) and H<sub>2</sub>O (mmol  
 341 H<sub>2</sub>O/mol air) concentrations in the system logger (1 s<sup>-1</sup>). Gap filling of missing data due to technical  
 342 problems (i.e., 27 % of the data across the study period between November 2015 and October 2016) was  
 343 based on the average diurnal cycle of each month.

344 The rates of soil CO<sub>2</sub> flux, R<sub>s</sub> (μmol CO<sub>2</sub> m<sup>-2</sup> s<sup>-1</sup>), were calculated from chamber data using a linear fit of  
 345 change in water-corrected CO<sub>2</sub> mole fraction using Eq. 4 (LiCor Manual, 2015) as follows:

$$346 \quad R_s = \frac{dC}{dt} \cdot \frac{vP}{sT_aR} \quad (4)$$

347 where dC/dt is the rate of change in the water-corrected CO<sub>2</sub> mole fraction (μmol CO<sub>2</sub> mol<sup>-1</sup> air s<sup>-1</sup>), v is  
 348 the system volume (m<sup>3</sup>), P is the chamber pressure (Pa), s is the soil surface area within the collar (m<sup>2</sup>), T<sub>a</sub>  
 349 is the chamber air temperature (K), and R is the gas constant (J mol<sup>-1</sup> K<sup>-1</sup>). A measurement period of 2  
 350 minutes was used, based on preliminary tests to obtain the most linear increase of CO<sub>2</sub> in the chambers  
 351 with the highest R<sup>2</sup>.

352 Soil CO<sub>2</sub> fluxes in the experimental plot were measured between November 2015 and October 2016 by  
 353 means of three measurement chambers using 21 collars grouped in seven sites in the forest stand, with  
 354 three locations (i.e., three collars) per site, based on different distances from the nearest tree (Dt). The  
 355 collars were inserted 5 cm into the soil. Data were recorded on a half-hour basis (48 daily records). The  
 356 three chambers were rotated between the seven sites every 1–2 weeks to cover all sites and to assess spatial  
 357 and temporal variations.

358 Upscaling of the collar measurements to plot-scale soil CO<sub>2</sub> flux was carried out by grouping collars based  
 359 on three locations (i.e., under trees [ $<1$  m from nearest tree; UT], in gaps between trees [1–2.3 m; BT], and  
 360 in open areas [ $>2.3$  m; OA]), with one chamber taking measurements at each location, and estimating the  
 361 fractional areas (Ø) of the three locations based on mapping the sites according to the distances noted  
 362 above, as previously done by Raz-Yaseef et al. (2010):

$$363 \quad R_s = R_{sOA} * \varnothing_{OA} + R_{sBT} * \varnothing_{BT} + R_{sUT} * \varnothing_{UT} \quad (5)$$

$$364 \quad \varnothing_{OA} + \varnothing_{BT} + \varnothing_{UT} = 1 \quad (6)$$

365 The annual scale of R<sub>s</sub> was derived from the upscaled chamber measurements (Eq. 5) based on daily  
 366 records (48 half-hourly values) of spatial upscaled R<sub>s</sub>.

367 Estimating the temperature sensitivity of R<sub>s</sub> (Q<sub>10</sub>) was performed as described by Davidson and Janssens  
 368 (2006) using a first-order exponential equation (see also Xu et al., 2015):

369 
$$R_s = a e^{bT_s} \quad (7)$$

370 where  $R_s$  represents the half-hour spatial upscaled time series of soil respiration flux ( $\mu\text{mol m}^{-2} \text{s}^{-1}$ ),  $T_s$   
 371 ( $^{\circ}\text{C}$ ) is soil temperature at a 5 cm depth (upscaled spatially and temporally using the same method as for  
 372  $R_s$ ), and  $a$  and  $b$  are fitted parameters. The  $b$  values were used to calculate the  $Q_{10}$  value according to the  
 373 following equation:

374 
$$Q_{10} = e^{10b} \quad (8)$$

#### 375 **2.4. Soil CO<sub>2</sub> flux partitioning**

376 Determination of different sources of soil CO<sub>2</sub> efflux was based on linear mixing models (Lin et al., 1999)  
 377 to estimate proportions for three main sources (autotrophic, heterotrophic, and abiotic), using isotopic  
 378 analysis of soil CO<sub>2</sub> profiles and soil incubation data from eight campaigns (January to September) during  
 379 2016, according to Equations 9–11. Partitioning of the monthly  $R_s$  values into components was done using  
 380 a 3-endmember triangular model for interpreting the  $\delta^{13}\text{C}$  and  $\Delta^{14}\text{C}$  values of CO<sub>2</sub> flux; the 3-endmember  
 381 triangular corners are the autotrophic ( $R_{sa}$ ), heterotrophic ( $R_h$ ), and abiotic ( $R_i$ ) sources of  $R_s$ . The  $\delta^{13}\text{C}$   
 382 and  $\Delta^{14}\text{C}$  isotope signatures of monthly  $R_s$  locate it inside the triangle (SI Fig. 2):

383 
$$\delta^{13}\text{C}_{R_s} = f_{sa} * \delta^{13}\text{C}_{sa} + f_h * \delta^{13}\text{C}_h + f_i * \delta^{13}\text{C}_i \quad (9)$$

384 
$$\Delta^{14}\text{C}_{R_s} = f_{sa} * \Delta^{14}\text{C}_{sa} + f_h * \Delta^{14}\text{C}_h + f_i * \Delta^{14}\text{C}_i \quad (10)$$

385 
$$1 = f_{sa} + f_h + f_i \quad (11)$$

386 where  $f$  indicates the fraction of total soil flux (e.g.,  $f_h=R_h/R_s$ ), while subscripts  $sa$ ,  $h$ , and  $i$  indicate  
 387 autotrophic, heterotrophic, and inorganic components, respectively. The three-equations system was used  
 388 to solve the three unknown  $f$  fractions of the total soil flux based on empirical estimates of the isotopic  
 389 endmembers. Additionally,  $\delta^{13}\text{C}$  and  $\Delta^{14}\text{C}$  are the stable and radioactive carbon isotopic ratios, where  $\delta^{13}\text{C}$   
 390  $= [([^{13}\text{C}/^{12}\text{C}]_{\text{sample}}/[^{13}\text{C}/^{12}\text{C}]_{\text{reference}})-1]*1000\text{‰}$  and the reference is the Vienna international standard  
 391 (VPDB). Radiocarbon data are expressed as  $\Delta^{14}\text{C}$  in parts per thousand or per mil (‰), which is the  
 392 deviation of a sample  $^{14}\text{C}/^{12}\text{C}$  ratio relative to the OxI standard in 1950 (see Taylor et al., 2015), that is,  
 393  $\Delta^{14}\text{C} = [([^{14}\text{C}/^{12}\text{C}]_{\text{sample}}/(0.95*[^{14}\text{C}/^{12}\text{C}]_{\text{reference}}*\exp[(y-1950)/8267]))-1]*1000\text{‰}$ , where  $y$  is the year of  
 394 sample measurements.

395 The  $\delta^{13}\text{C}_{R_s}$  was estimated monthly using the Keeling plot approach (SI Figs 3 and 4; Pataki et al., 2003;  
 396 Taneva and Gonzalez-Meler, 2011). Soil air was sampled using closed-end stainless steel tubes (6 mm  
 397 diameter) perforated near the tube bottom at four depths (30, 60, 90, and 120 cm). Samples of soil air were  
 398 collected in pre-evacuated 150 mL glass flasks with high-vacuum valves, the dead volume in the tubing  
 399 and flask necks having been purged with soil air using a plastic syringe equipped with a three-way valve.

400 Note that the Keeling plot approach is based on the 2-endmembers mixing model (see Review of Pataki et  
401 al., 2003), which often does not hold in soils because of variations in the  $\delta^{13}\text{C}$  values of source material  
402 with depth (see a recent example in Joseph et al., 2019). However, probably because of the very dry  
403 conditions at our study site, no change in  $\delta^{13}\text{C}$  with depth in the root zone is observed ( $\pm 0.1\%$  across the  
404 35 cm depth profiles; SI Fig. 5), providing an opportunity to avoid this caveat, we must also conclude of  
405 course that the variations among the contributions of Rsa, Rh, and Ri do not change significantly with  
406 depth and permitting the use of the single set of isotopic signatures in Table 2. The soil  $\text{CO}_2$  samplings  
407 carried out therefore represented predominantly the mixing of atmospheric  $\text{CO}_2$  with a single integrated  
408 soil source signal, consistent with the Keeling plot approach.

409 The autotrophic ( $\delta^{13}\text{C}_{\text{sa}}$ ) endmember was estimated based on incubations during the sampling periods of  
410 excised roots, following Carbone et al. (2008). Fine roots (<2 mm diameter) were collected, rinsed with  
411 deionized water, and incubated for 3 hours in 10 mL glass flasks connected with Swagelok Ultra-Torr tee  
412 fittings to 330 mL glass flasks equipped with Louwers high-vacuum-valves. The flasks were flushed with  
413  $\text{CO}_2$ -free air at room temperature close to field conditions. The  $\text{CO}_2$  was allowed to accumulate to at least  
414 2,000 ppm (~2 h).

415 The heterotrophic ( $\delta^{13}\text{C}_{\text{h}}$ ) endmember was estimated as in Taylor et al. (2015), and, similar to the root-  
416 incubation experiment, soil samples from the top 5 cm of the litter layer or 10 cm below the soil surface  
417 were collected, and roots were carefully removed to isolate heterotrophic components. Root-free soils were  
418 placed in 10 mL glass flasks and allowed to incubate for 24 hours before being transferred to evacuated  
419 330 mL glass flasks. The inorganic source ( $\delta^{13}\text{C}_{\text{i}}$ ) endmember was estimated using one gram of dry soil  
420 (ground to pass through a 0.5 mm mesh) placed in a 10 mL tube with a septum cap; then, 12 mL of 1M  
421 HCl was added to dissolve the carbonate fraction, and the fumigated  $\text{CO}_2$  withdrawn from each tube was  
422 collected using a 10 mL syringe and injected into a 330 mL evacuated flask for isotopic analysis.

423 Radiocarbon estimates were based on the work of Carmi et al. (2013) at the same site, adjusted to the  
424 measured atmospheric  $^{14}\text{C}$  values during the study period (49.5‰; Carmi et al., 2013). The  $\Delta^{14}\text{C}_{\text{sa}}$  and  
425  $\Delta^{14}\text{C}_{\text{h}}$  endmembers were estimated based on the assumption that they carry the  $^{14}\text{C}$  signatures of 4 and 8.5  
426 years, respectively, older than the  $^{14}\text{C}$  signature of the atmosphere at the time of sampling, based on mean  
427 ages previously estimated (Graven et al., 2012; Levin et al., 2010; Taylor et al., 2015).  $\Delta^{14}\text{C}_{\text{i}}$  was obtained  
428 from Carmi et al. (2013). Monthly values of  $\Delta^{14}\text{C}_{\text{Rs}}$  were obtained using the linear equation of the  
429 regression line of the measured  $\delta^{13}\text{C}$  values of Rsa, Rsh, and Ri and the corresponding estimated  $\Delta^{14}\text{C}$   
430 values (SI Fig. 2) and monthly  $\delta^{13}\text{C}$  values of Rs.

## 431 **2.5. Isotopic analysis**

432 Isotopic analysis followed the methodology described in Hemming et al. (2005). The  $\delta^{13}\text{C}$  of  $\text{CO}_2$  in the  
433 air was analyzed using a continuous flow mass spectrometer connected to a 15-flask automatic manifold  
434 system. An aliquot of 1.5 mL of air was expanded from each flask into a sampling loop on a 15-position  
435 valve (Valco Houston, TX, USA).  $\text{CO}_2$  was cryogenically trapped from the air samples using helium as a  
436 carrier gas; it was then separated from  $\text{N}_2\text{O}$  with a Carbosieve G (Sigma Aldrich) packed column at  $70^\circ\text{C}$   
437 and analyzed on a Europa 20-20 Isotope Ratio Mass Spectrometer (Crewe, UK).  $\delta^{13}\text{C}$  results were quoted  
438 in parts per thousand (‰) relative to the VPDB international standard. The analytical precision was  
439 0.1‰. To measure  $[\text{CO}_2]$ , an additional 40.0 mL subsample of air from each flask was expanded into  
440 mechanical bellows and then passed through an infrared gas analyzer (LICOR 6262; Lincoln, NE, USA)  
441 in an automated system. The precision of these measurements was 0.1 ppm. Flasks filled with calibrated  
442 standard air were measured with each batch of 10 sample flasks; five standards were measured per 10  
443 samples for  $\delta^{13}\text{C}$  analyses and four standards per 10 samples for  $[\text{CO}_2]$  analyses.

444 Organic matter samples were dried at  $60^\circ\text{C}$  and milled using a Wiley Mill fitted with size 40 mesh, and  
445 soil samples were ground in a pestle and mortar. Soils containing carbonates were treated with 1M  
446 hydrochloric acid. Between 0.2 and 0.4 mg of each dry sample was weighed into tin capsules (Elemental  
447 Microanalysis Ltd., Okehampton, UK), and the  $\delta^{13}\text{C}$  of each was determined using an elemental analyzer  
448 linked to a Micromass Optima IRMS (Manchester, UK). Three replicates of each sample were analyzed,  
449 and two samples of a laboratory working standard cellulose were measured for every 12 samples. Four  
450 samples of the acetanilide (Elemental Microanalysis Ltd.) international standard were used to calibrate  
451 each run, and a correction was applied to account for the influence of a blank cup. The precision was  
452 0.1‰.

## 453 2.6. Total belowground carbon allocation (TBCA)

454 TBCA ( $\text{g C m}^{-2} \text{ y}^{-1}$ ) was calculated following Giardina and Ryan (2002) for the study year (November  
455 2015–October 2016) as follows:

$$456 \quad \text{TBCA} = R_s - R_{\text{alp}} + \Delta C_{\text{soil}} \quad (12)$$

457 where  $R_{\text{alp}}$  is the annual aboveground litter production between November 2014 and October 2015, and  
458  $\Delta C_{\text{soil}}$  is the annual change in belowground total soil organic C. Litter production, not measured during the  
459 present study, was estimated based on values obtained by Masyk et al. (2008b) for 2000–2006 ( $56 \text{ g C m}^{-2} \text{ y}^{-1}$ )  
460 and assumed to have increased in the study period (2014–2015) proportionally to the measured  
461 increase in leaf area index (LAI; 1.31 to 1.94; i.e.,  $R_{\text{alp}} = [(1.94*56)/1.31] = 83 \text{ g C m}^{-2} \text{ y}^{-1}$ ). For  
462 herbaceous litter production, three plots of  $25 \text{ m}^2$  were randomly selected in 2002 and harvested at the end  
463 of the growing season, total fresh biomass was weighed, and subsamples were used to determine dry weight

464 and C content. Grünzweig et al. (2007) found that herbaceous litter production was close to the average  
465 rainfall for the specific year; this method was adapted in the current study for the period between November  
466 2014 and October 2015. Since aboveground litter ( $R_{alp}$ ; the sum of tree litter and herbaceous litter  
467 production) of a given year was mainly produced during that year but decayed during the following  
468 hydrological year, TBCA was on the current year's  $R_s$  (2015–2016) and the previous year's  $R_{alp}$  (2014–  
469 2015).  $\Delta C_{soil}$  was set constant as the average annual belowground carbon increase since afforestation  
470 (Qubaja et al., in press).

## 471 2.6. Statistical analyses

472 Two-way ANOVA tests were performed at a significance level set at  $p = 0.001$  to detect significant effects  
473 of locations (OA, BT, and UT), sites, and their interactions on  $R_s$  and meteorological parameters. Pearson  
474 correlation analysis ( $r$ ) was used to detect the correlation between  $R_s$  and meteorological parameters. To  
475 quantify spatio-temporal variability in  $R_s$ , the coefficient of variation (CV%) was calculated as  
476  $[(STDEV/Mean)*100\%]$ . Heterogeneity was considered weak if  $CV\% \leq 10\%$ , moderate if  $10\% < CV\% \leq$   
477  $100\%$ , and strong if  $CV\% > 100\%$ . All the analyses were performed using Matlab software, Version  
478 R2017b (MathWorks, Inc., MA, USA).

## 479 3. Results

### 480 3.1. Spatial variations

481 The spatial variations in  $R_s$  across locations (distance from nearest tree) and sites (across the study area)  
482 are reported in Table 1, together with other measured variables. The results indicated an overall mean  $R_s$   
483 value of  $0.8 \pm 0.1 \mu\text{mol m}^{-2} \text{s}^{-1}$ , with distinct values for the three locations.  $R_s$  was greater at UT locations  
484 than at the BT and OA locations by a factor of  $\sim 2$ . The spatial variability among the locations was also  
485 apparent in the  $R_s$  daily cycle (Fig. 1), with clear differences between the wet season (November to April),  
486 when the UT showed consistently higher  $R_s$  values than at other locations by a factor of about 1.6 and the  
487 dry season by a factor of approximately 2.6. Note that the daily peak in  $R_s$  remained at midday in both the  
488 wet and dry seasons. Overall, the 21 collars showed moderate variations ( $CV = 55\%$ ; Table 1),  $R_s$  was  
489 negatively correlated with distance from trees ( $D_t$ ;  $r = -0.62$ ;  $p < 0.01$ ) and with soil and air temperatures  
490 ( $T_s$  and  $T_a$ ;  $r = -0.45$ ;  $p < 0.05$ ), and positively correlated with soil water content and relative humidity  
491 (SWC and RH;  $r = 0.50$ ;  $p < 0.05$ ). The inverse correlation between  $R_s$  and distance from the nearest tree  
492 could be useful in considering the expected decline in stand density due to thinning and mortality (e.g.,  
493 associated with a drying climate). For a first approximation, the results indicate that decreasing from the

494 present stand density of 300 trees ha<sup>-1</sup> to 100 trees ha<sup>-1</sup> and the resulting increase in mean distance among  
495 trees could result in decreasing ecosystem Rs by 11%.

496

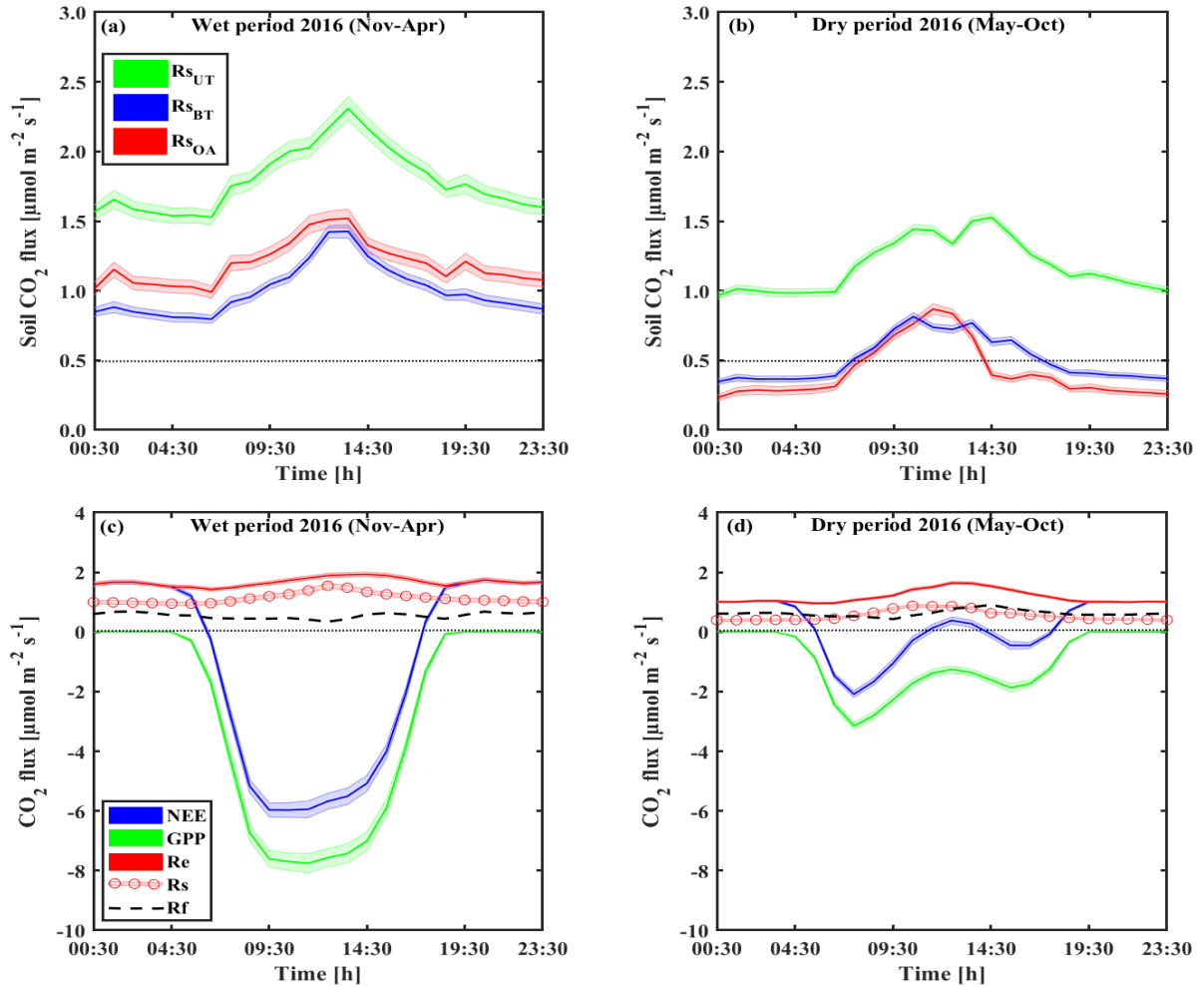
497 **Table 1** Annual mean of half-hour values across locations (OA, open area; BT, between trees; UT, under tree) in  
 498 seven sites in the forest during the study period, of soil respiration flux rates (Rs) together with the soil water content  
 499 at 10 cm depth (SWC), minimum distances from nearby tree (Dt), soil temperature at 5 cm depth (Ts), and air  
 500 temperature (Ta) and relative humidity (RH) at the soil surface (numbers in parenthesis indicate  $\pm$ se).

Locations	Sites	Rs [ $\mu\text{mol m}^{-2} \text{s}^{-1}$ ]	SWC [x100 m <sup>3</sup> m <sup>-3</sup> ]	Dt [m]	Ts [°C]	Ta [°C]	RH [%]
OA	1	1.64 (0.02)	16.5 (0.2)	2.9	15.6 (0.1)	15.4 (0.2)	59.7 (0.5)
	2	0.72 (0.01)	14.5 (0.2)	3.6	15.9 (0.2)	15.0 (0.2)	58.4 (0.6)
	3	1.23 (0.02)	19.3 (0.2)	7.0	20.6 (0.3)	18.2 (0.2)	53.5 (0.5)
	4	0.38 (0.01)	11.3 (0.2)	3.0	22.6 (0.2)	20.8 (0.1)	58.9 (0.4)
	5	0.38 (0.01)	5.8 (0.2)	3.0	25.5 (0.1)	24.0 (0.1)	43.1 (0.4)
	6	0.31 (0.01)	5.7 (0.4)	2.8	30.0 (0.3)	26.2 (0.3)	51.8 (0.9)
	7	0.14 (0.01)	6.1 (0.3)	3.5	25.5 (0.2)	23.2 (0.3)	44.5 (0.9)
	<b>Average</b> <b>CV [%]</b>	<b>0.68 (0.21)</b> <b>81 %</b>	<b>11 (0)</b> <b>50%</b>	<b>3.7 (0.6)</b> <b>41%</b>	<b>22.3 (2.0)</b>	<b>20.4 (1.6)</b>	<b>52.8 (2.6)</b> <b>13 %</b>
BT	1	0.77 (0.01)	10.5 (0.2)	1.8	16.1 (0.1)	15.2 (0.2)	60.5 (0.5)
	2	0.88 (0.01)	12.1 (0.2)	1.5	14.8 (0.2)	14.7 (0.2)	59.5 (0.6)
	3	0.84 (0.01)	20.4 (0.2)	2.7	20.1 (0.3)	18.4 (0.2)	54.1 (0.6)
	4	0.91 (0.01)	14.4 (0.2)	2.7	23.3 (0.2)	21.3 (0.2)	58.5 (0.4)
	5	0.41 (0.00)	3.9 (0.2)	2.0	24.6 (0.1)	24.0 (0.1)	43.2 (0.4)
	6	0.41 (0.01)	3.3 (0.4)	2.5	29.1 (0.2)	26.0 (0.3)	52.5 (0.8)
	7	0.46 (0.01)	5.5 (0.3)	1.2	23.9 (0.1)	22.8 (0.3)	45.7 (0.9)
	<b>Average</b> <b>CV [%]</b>	<b>0.67 (0.09)</b> <b>35 %</b>	<b>10 (0)</b> <b>63%</b>	<b>2.0 (0.2)</b> <b>29%</b>	<b>21.7 (1.9)</b>	<b>20.3 (1.6)</b>	<b>53.4 (2.6)</b> <b>13 %</b>
UT	1	1.22 (0.02)	9.3 (0.2)	0.2	15.7 (0.1)	15.2 (0.2)	60.0 (0.5)
	2	1.42 (0.01)	14.0 (0.2)	0.3	14.8 (0.2)	14.8 (0.2)	59.4 (0.6)
	3	1.64 (0.01)	19.8 (0.2)	0.5	19.0 (0.2)	18.0 (0.2)	54.5 (0.6)
	4	1.90 (0.02)	11.3 (0.2)	0.6	22.0 (0.1)	20.8 (0.1)	59.0 (0.4)
	5	1.16 (0.01)	4.0 (0.2)	0.4	23.9 (0.1)	23.7 (0.1)	44.1 (0.4)
	6	1.29 (0.01)	4.5 (0.4)	0.2	29.5 (0.3)	25.9 (0.3)	52.7 (0.9)
	7	0.89 (0.01)	5.2 (0.3)	0.2	25.0 (0.1)	23.0 (0.3)	45.5 (0.9)
	<b>Average</b> <b>CV [%]</b>	<b>1.36 (0.13)</b> <b>25 %</b>	<b>10 (0)</b> <b>60%</b>	<b>0.3 (0.1)</b> <b>46%</b>	<b>21.4 (2.0)</b>	<b>20.2 (1.6)</b>	<b>53.6 (2.5)</b> <b>12 %</b>
All	<b>Average (SE)</b>	<b>0.8 (0.1)</b>	<b>11 (0)</b>	<b>2.0 (0.4)</b>	<b>21.8 (1.1)</b>	<b>20.3 (0.9)</b>	<b>53.3 (1.4)</b>
	<b>Max</b>	<b>1.90</b>	<b>20</b>	<b>7.0</b>	<b>30.0</b>	<b>26.2</b>	<b>60.5</b>
	<b>Min</b>	<b>0.14</b>	<b>3</b>	<b>0.2</b>	<b>14.8</b>	<b>14.7</b>	<b>43.1</b>
	<b>CV [%]</b>	<b>55 %</b>	<b>55%</b>	<b>82%</b>			<b>12 %</b>
Two-way ANOVA (P value)	Site	<b>0.000</b>	<b>0.000</b>		<b>0.000</b>	<b>0.000</b>	<b>0.000</b>
	Location	<b>0.000</b>	<b>0.000</b>		<b>0.000</b>	<b>0.220</b>	<b>0.074</b>
	Site x Location	<b>0.000</b>	<b>0.000</b>		<b>0.000</b>	<b>0.645</b>	<b>0.961</b>
<b>Pearson Correlation with Rs</b>			<b>.50*</b>	<b>-.62**</b>	<b>-.45*</b>	<b>-.45*</b>	<b>.50*</b>

501 \*\* . Correlation is significant at the 0.01 level (two-tailed).

502 \* . Correlation is significant at the 0.05 level (two-tailed).





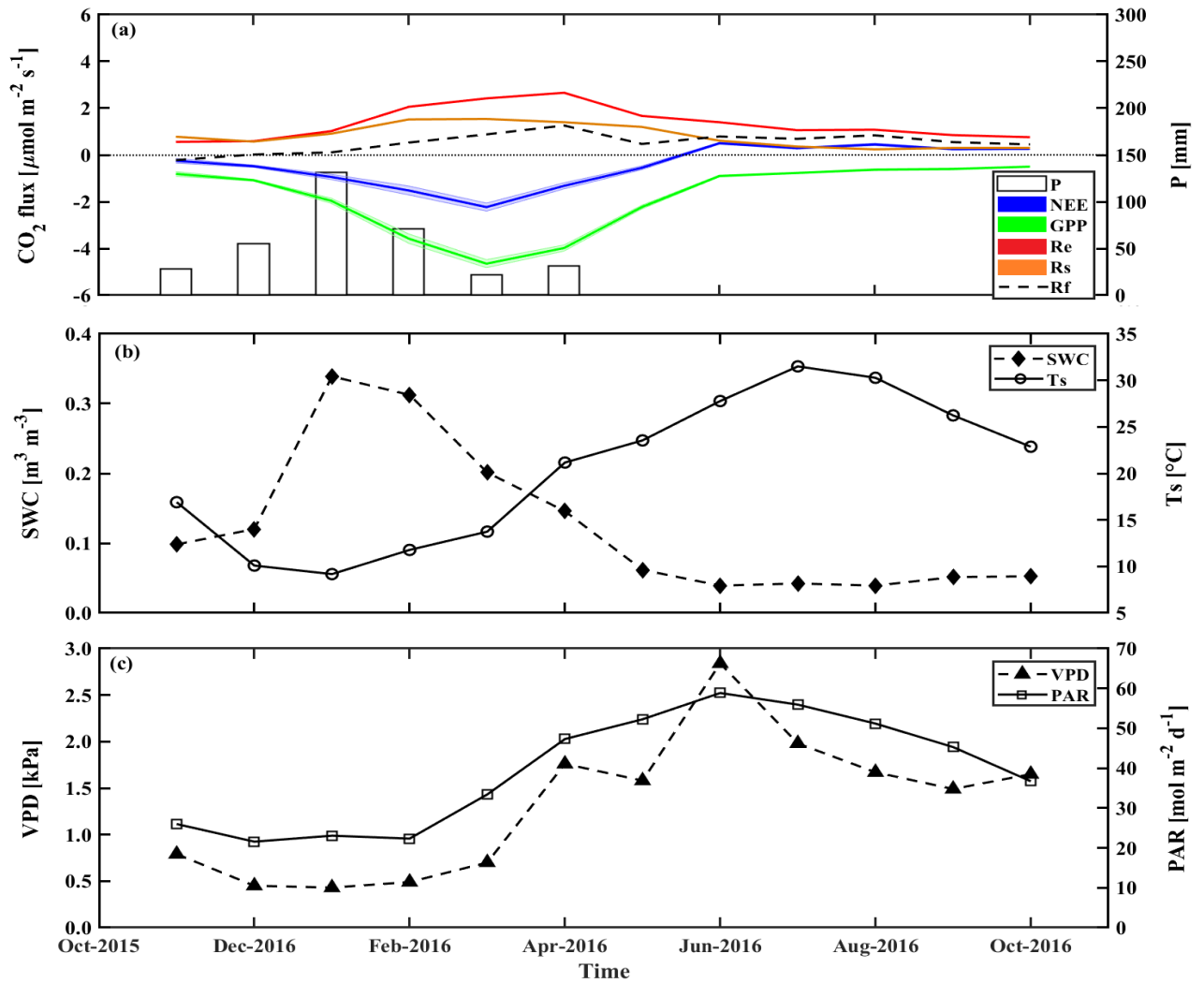
503  
 504 **Figure 1** Representative diurnal cycles of soil respiration (Rs; using soil chambers across locations: open area, OA;  
 505 between trees, BT; under trees, UT) and sites in panels a and b, of net ecosystem exchange (NEE; canopy scale eddy  
 506 covariance) and gross primary production (GPP), and ecosystem respiration (Re) and its partitioning to soil respiration  
 507 (Rs) and aboveground tree respiration (Rf) in panels c and d, during the wet (Nov–Apr) and dry (May–Oct)  
 508 periods. Based on half-hour values over the diurnal cycle; shaded areas indicate  $\pm se$ ; Rf was estimated as the residual as  $R_f =$   
 509  $Re - R_s$  and was presented as a dashed line.

### 510 3.2. Temporal dynamics

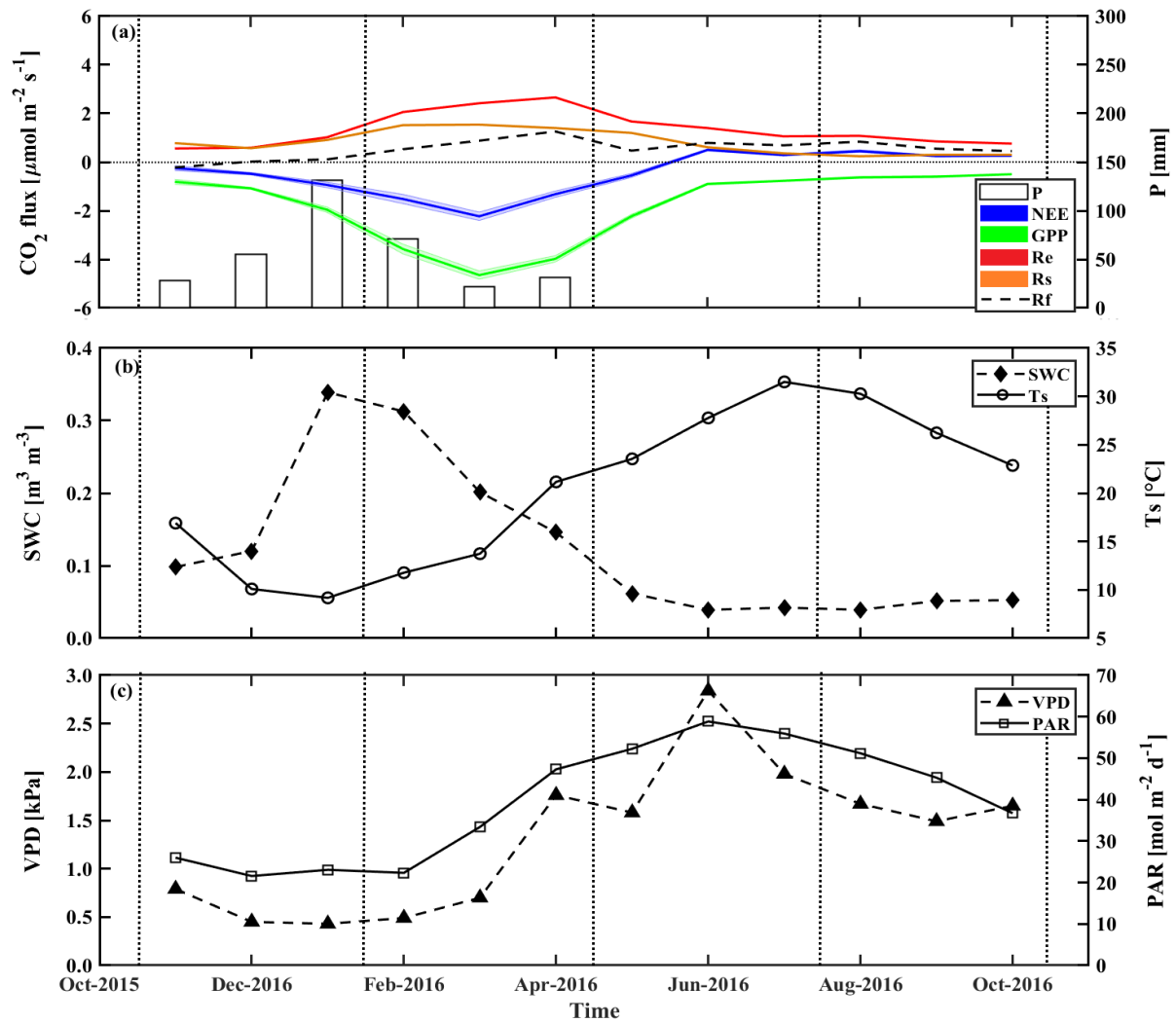
511 On the diurnal timescale, CO<sub>2</sub> fluxes showed typical daily cycles (Fig. 1). As expected, on average, all CO<sub>2</sub>  
 512 fluxes were higher during the wet period compared to the dry season by a factor of ~2. However, Rs and  
 513 Re peaked around midday in both the wet and dry seasons, while the more physiologically controlled NEE  
 514 and GPP showed a shift from midday (around 11:00–14:00) to early morning (08:00–11:00) in the dry  
 515 season, with a midday depression and a secondary afternoon peak (Fig. 1d).

516 The temporal variations across the seasonal cycle are reported in Fig. 2, based on monthly mean values,  
 517 exhibiting sharp differences between the wet and dry seasons. As previously observed in this semi-arid  
 518 site, all CO<sub>2</sub> fluxes peak in early spring between March and April. The corresponding high-resolution data

519 are reported in SI Fig. 6, which show also that the high winter (February)  $R_s$  rates were associated with  
 520 clear days when photosynthetic active radiation (PAR) increased with air temperature,  $T_a$ . These data also  
 521 show that, following rainy days, daily  $R_s$  values could reach  $6.1 \mu\text{mol m}^{-2} \text{s}^{-1}$  (i.e., in the UT microsite;  
 522 [data not shown](#)), although the average was  $1.1 \pm 0.2 \mu\text{mol m}^{-2} \text{s}^{-1}$  during the wet period, which diminished  
 523 by  $\sim 55\%$  in the dry season to mean daily values of  $0.5 \pm 0.1 \mu\text{mol m}^{-2} \text{s}^{-1}$ . In spring (April), all  $\text{CO}_2$  fluxes  
 524 peaked during the crossover trends of decreasing soil moisture content and increasing both temperature  
 525 and PAR (SI Fig. 6).



526



527

528 **Figure 2** Seasonal trends of monthly mean values during the research period of a) the fluxes of net ecosystem  
 529 exchange (NEE), gross primary production (GPP), and ecosystem respiration (Re) and its components, soil respiration  
 530 (Rs) and aboveground tree respiration (Rf); and monthly mean of key environmental parameters, b) soil water content  
 531 at the top 10 cm (SWC<sub>0-10</sub>) and soil temperature at 5 cm (Ts), and c) vapor pressure deficit (VPD) and photosynthetic  
 532 activity radiation (PAR). Rf is obtained from the Re-Rs. [Vertical dotted lines indicate the winter, spring, summer and](#)  
 533 [autumn seasons.](#)

534 The temporal variations in the half-hour values of Rs reflected changes in soil moisture at 0–5 cm depth  
 535 and PAR ( $r = 0.5$  and  $0.2$ , respectively;  $p < 0.01$ ) and negative correlations with Ts and RH ( $r = 0.2$  and  
 536  $0.1$ , respectively;  $p < 0.01$ ). The variations in the integrated Rs showed a CV of 71%, with the temporal  
 537 variations dominated strongly by PAR (CV > 100%), moderately by SWC (CV~85%), and weakly by RH  
 538 (CV~40%)[\(correlations and CV values were not included in figures and tables\).](#) Repeating the models  
 539 applied by Grünzweig et al. (2009), the potential climatic factors that best predicted daily Rs shifted from  
 540 SWC and PAR in the dry season to Ts and PAR in the wet season (SI Table 2). These equations explained  
 541 43% and 70% of the variation in Rs in the dry and wet seasons, respectively (SI Table 2). A reasonable

542 forecast of the temporal variations in  $R_s$  ( $\mu\text{mol m}^{-2} \text{s}^{-1}$ ) at half-hour values ( $R^2 = 0.60$ ,  $p < 0.0001$ ) was  
 543 obtained based on  $\text{SWC}_{0-10}$  and  $T_s$  values across the entire seasonal cycle, based on:

$$544 \quad R_s = 0.05126 * \exp(0.04274 * T_s + 28.51 * \text{SWC} - 74.44 * \text{SWC}^2) \quad (13)$$

545 At the ecosystem scale,  $R_e$  was characterized by high fluxes in the wet season and peak values of  $\sim 2.4$   
 546  $\mu\text{mol m}^{-2} \text{s}^{-1}$  in February to April (Fig. 2; SI Table 1). [Refluxes](#)[Re fluxes](#) rapidly decreased after the  
 547 cessation of rain and reached the lowest values in the fall (September to October), with mean dry period  
 548 values of  $0.5 \pm 0.1 \mu\text{mol m}^{-2} \text{s}^{-1}$  (Fig. 2, SI Table 1). GPP had a mean value of  $-1.8 \pm 0.4 \mu\text{mol m}^{-2} \text{s}^{-1}$ , and  
 549 daily NEE had a mean value of  $-0.5 \pm 0.3 \mu\text{mol m}^{-2} \text{s}^{-1}$  (SI Table 1 and SI Fig. 6), with the same seasonality  
 550 (Fig. 2).

551 **Table 2**  $\delta^{13}\text{C}$  and  $\Delta^{14}\text{C}$  signature of soil respiration ( $R_s$ ) and its partitioning to autotrophic ( $R_{sa}$ ), heterotrophic ( $R_h$ ),  
 552 and abiotic ( $R_i$ ), together with the relative contribution of each to the soil and ecosystem respiration for Yatir forest  
 553 during eight campaigns of measurements from January to September 2016 (numbers in parenthesis indicate  $\pm$ se) in  
 554 comparison to results obtained previously in the same forest (2001–2006 mean values). The monthly contribution of  
 555  $R_{sa}$ ,  $R_h$ , and  $R_i$  to  $R_s$  or  $R_e$  is presented in Fig. 3a and b, respectively.

Signature	$R_{sa}$	$R_h$	$R_i$	$R_s$
	[%]			
$\delta^{13}\text{C}$	-23.7 (0.5) <sup>1</sup>	-24.3 (0.0) <sup>1</sup>	-6.5 (0.0) <sup>1</sup>	-20.8 ( $\pm 0.6$ ) <sup>1</sup>
$\Delta^{14}\text{C}$	30 <sup>3</sup>	50 <sup>3</sup>	-900 <sup>2</sup>	-134 (34) <sup>4</sup>
<b>Relative contribution to <math>R_s</math> (2015–2016)</b>	<b>0.40 (0.02)</b>	<b>0.39 (0.02)</b>	<b>0.21 (0.04)</b>	
<b>Relative contribution to <math>R_e</math> (2015–2016)</b>	<b>0.24 (0.04)</b>	<b>0.23 (0.04)</b>	<b>0.13 (0.01)</b>	<b>0.60 (0.06)</b>

556 <sup>1</sup> Measured in the present study; <sup>2</sup> measured by Carmi et al., (2013); <sup>3</sup> calculated based on the measured atmospheric  
 557 value by Carmi et al. (2013); and <sup>4</sup> calculated based on the best fit regression equation in SI Fig. 2.

558 Figure 3 (see also Table 2) summarizes the seasonal variations in  $R_s$  and  $R_e$  partitioning. The monthly  $R_{sa}$   
 559 and  $R_h$  were not significantly different but were significantly different from  $R_i$  ( $p < 0.05$ ). The  $R_{sa}/R_s$   
 560 ratios ranged from 0.32 to 0.46, the largest contribution occurring in early spring from February to April.  
 561 The  $R_h/R_s$  fraction ranged between 0.33 and 0.45, being [the](#) highest during the wet season. The  $R_i/R_s$  –  
 562 the fraction of inorganic sources from the total soil respiration – ranged from 0.09 to 0.35, the largest  
 563 contribution being in the driest period. The mean relative contributions of these components to  $R_s$  over the  
 564 sampling campaigns are presented in Figure 3a, but, on average, soil biotic fluxes were higher than abiotic  
 565 fluxes by a factor of  $\sim 4$ . [Repartitioning](#)[Re partitioning](#) showed an average increase in  $R_f/R_e$  from 25% in  
 566 the wet season to 54% in the dry season and a decline in  $R_s/R_e$  from 75% to 46% on average in the wet  
 567 and the dry seasons, respectively, which reflected a seasonal change of  $R_f$  in the wet season to peak values  
 568 in the dry season (Fig. 3b). Both the highest and lowest  $R_s$  fractions ( $\sim 0.74$  and nearly 0.34) along the  
 569 seasonal cycle were associated with low total  $R_e$  fluxes, that is, in the fall before the  $R_f$  peak in the spring  
 570 and in the summer, when physiological controls limited water loss ([Fig. 2](#)).

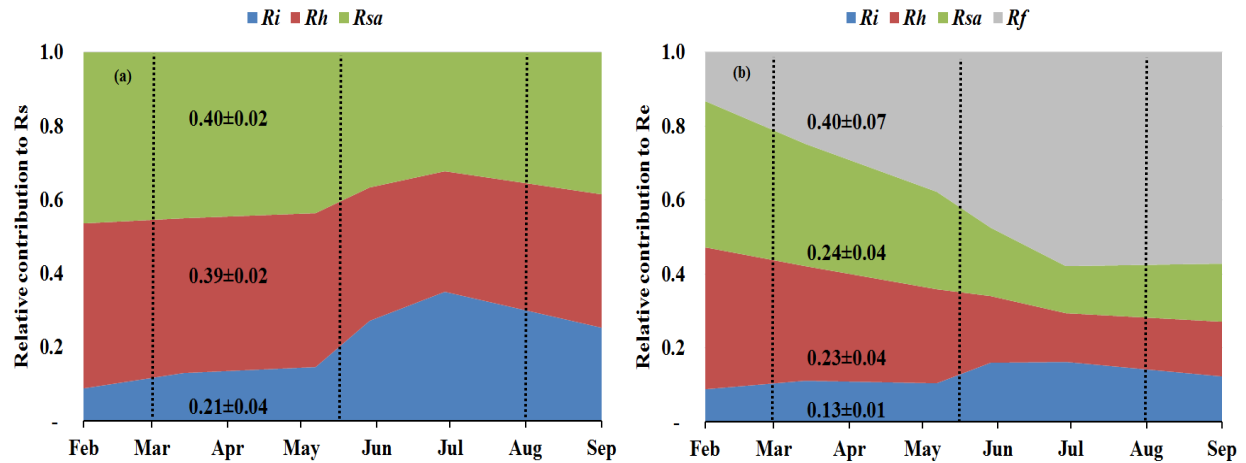


**Figure 3** a) Linear mixing models  $\delta^{13}\text{C}$  and  $\Delta^{14}\text{C}$  of soil respiration ( $R_s$ ) isotope signatures (from soil  $\text{CO}_2$  profile method at 0, 30, 60, 90, and 120 cm soil depth) were used to determine the seasonal variations in the relative contribution of soil autotrophic ( $R_{sa}$ ), heterotrophic ( $R_h$ ), and abiotic ( $R_i$ ) components to  $R_s$ , and b) seasonal variations in the relative contribution of soil autotrophic ( $R_{sa}$ ), heterotrophic ( $R_h$ ), abiotic ( $R_i$ ), and foliage and stem respiration ( $R_f$  is obtained from the  $R_e - R_s$ ) components to ecosystem respiration ( $R_e$ ) during eight campaigns (Jan–Sep) in 2016. The contributions were estimated with linear mixing models using  $\delta^{13}\text{C}$  and  $\Delta^{14}\text{C}$  of soil respiration ( $R_s$ ) and of soil  $\text{CO}_2$  profile method at 0 to 120 cm soil depth. Vertical dotted lines indicate the winter, spring, summer and autumn seasons. These results confirmed earlier estimates of Grünzweig et al. (2009) and Maseyk et al. (2008a).

571  
572  
573  
574  
575  
576  
577  
578  
579  
580

### 581 3.3. Annual scale

**Table 3** Mean annual values of ecosystem respiration ( $R_e$ ), its components and associated ratios, net ecosystem exchange (NEE; from eddy covariance), net primary productivity (NPP), gross primary productivity (GPP), carbon-use efficiency (CUE), leaf area index (LAI), and ratio of total belowground carbon allocation (TBCA) to GPP (TBCA/GPP) in the present study (mean of Nov 2015 to Oct 2016) and in comparison to results obtained previously in the same forest (2001–2006 mean values).  $R_i$ ,  $R_h$ ,  $R_{sa}$ ,  $R_s$ ,  $R_l$  and  $R_w$  denote abiotic, heterotrophic, soil autotrophic, soil, foliage, and wood  $\text{CO}_2$  flux, respectively.  $Q_{10}$  is derived during the two studies for the wet and dry season.

Study	$R_s$	$R_h$	$R_{sa}$	$R_l$	$R_w$	$R_i$	$R_e$	NEE	NPP	GPP
Mean (2001–2006)	406	147	203	260	70	56	735	-211	-358	-880
$x/R_s$		0.36	0.50			0.14				
$x/R_e$	0.55	0.20	0.28	0.35	0.10	0.07				
Mean (2015–2016)	295	115	119	155	39	61	488	-167	-282	-655
$x/R_s$		0.39	0.40			0.21				
$x/R_e$	0.60	0.23	0.24	0.32	0.08	0.13				
Ratio of $(x/R_s)_{2016}/(x/R_s)_{2003}$		<b>1.08</b>	<b>0.81</b>			<b>1.50</b>				
Ratio of $(x/R_e)_{2016}/(x/R_e)_{2003}$	<b>1.09</b>	<b>1.18</b>	<b>0.88</b>	<b>0.90</b>	<b>0.84</b>	<b>1.64</b>				

Study	$Q_{10}$		CUE	TBCA/GPP <sup>3</sup>	LAI [m <sup>2</sup> m <sup>-2</sup> ]
	SWC <sup>1</sup>	SWC <sup>2</sup>			
Mean (2001–2006)	2.5	1.2	0.40	0.41	1.3
Mean (2015–2016)	1.6	1.1	0.43	0.38	2.1
Ratio of $x_{2016}/x_{2003}$	<b>0.64</b>	<b>0.92</b>	<b>1.06</b>	<b>0.93</b>	<b>1.62</b>

589  
590  
591

<sup>1</sup> SWC  $\geq 0.2$  [m<sup>3</sup> m<sup>-3</sup>] and <sup>2</sup> SWC  $< 0.2$  [m<sup>3</sup> m<sup>-3</sup>]; <sup>3</sup> and the mean of GPP used by Grünzweig et al., 2009 to estimate the TBCA/GPP was 834 g m<sup>-2</sup> y<sup>-1</sup>.

592 On an annual timescale, estimates of CO<sub>2</sub> flux components based on EC measurements resulted in annual  
593 values of GPP, NPP, Re, and NEP of 655, 282, 488, and 167 g C m<sup>-2</sup> y<sup>-1</sup>, respectively (Tables 3 and SI-1).  
594 On average across the measurement period, Rs was the main CO<sub>2</sub> flux to atmosphere, making up 60 ± 6%  
595 of Re (295 ± 4 g C m<sup>-2</sup> y<sup>-1</sup>; Tables 3 and SI-1), and Rf was another significant component accounting for  
596 40 ± 6% of Re (Fig. 3b), which reflected the low density (300 trees ha<sup>-1</sup>) nature of the semi-arid forest. As  
597 indicated above, Re partitioning showed a decrease in Rs/Re and an increase in Rf/Re from winter to  
598 summer, which is clearly apparent in Fig. 3b. On an annual scale, during the study period, estimates of Rf,  
599 Rsa, Rh, and Ri values were 194 ± 36, 119 ± 21, 115 ± 20, and 61 ± 6 g C m<sup>-2</sup> y<sup>-1</sup>, respectively. ~~Despite~~  
600 ~~relatively high~~ These rates of respiration fluxes, ~~the CUE of translated at~~ the ecosystem ~~remained high~~  
601 ~~at scale to Re/GPP of ~75%, lower than observed in other ecosystems (SI Table 3) and leading, in turn, to~~  
602 ~~high ecosystem CUE of 0.43.~~

603 Using the site records of nearly 20 years, long-term trends in GPP, NPP, Re, and NEP were  
604 ~~obtained~~ examined. Soil respiration and its partitioning could not be similarly monitored continuously, but  
605 combining the present results with the 2001–2006 values obtained by Grünzweig et al. (2009) and Maseyk  
606 et al. (2008a) provided a basis for estimating the long-term trends in soil respiration. Notably, no clear or  
607 significant trend over time was observed in any of the canopy-scale continuously monitored fluxes, but,  
608 because of relatively large interannual variations, associated mainly with those in precipitation (see Qubaja  
609 et al., in press), it is likely that the relative contributions of the different fluxes, expressed as ratios in Table  
610 3, provide a more robust perspective of the long-term temporal changes in the ecosystem functioning. The  
611 results presented ~~in~~ Table 3 reflect the long-term growth of the forest, with a relatively large increase in  
612 LAI, but the ~~belowground allocation~~ TBCA remained around 40%. The ~~ratio of the respiration components~~  
613 ~~to total ecosystem respiration, Re, or to GPP~~ results also indicated little change in the total soil respiration,  
614 Rs, component, ~~(as a fraction of Re or GPP),~~ but a general shift from the autotrophic components ~~Rsa, Rl,~~  
615 ~~and Rw~~ to the heterotrophic component ~~(i.e., Rh).~~ This was reflected in the decreasing ratio of the  
616 ~~autotrophic components (i.e., Rsa, Rl, and Rw) to Re, and the increasing ratio of Rh (Table 3)~~ across the  
617 13-year observation period ~~noted above (with the mean values for 2011–2005 assigned to (2003 and the~~  
618 ~~new data~~ to 2016).

#### 619 4. Discussion

620 Partitioning ecosystem carbon fluxes and long-term observational studies are key to understanding  
621 ecosystem carbon dynamics and their response to change. Overall, the results support our research  
622 hypothesis that the observed high CUE at our site is at least partly due to the characteristics of the carbon  
623 flux partitioning that can be associated with the semi-arid conditions. Compared to other sites and climates  
624 (see comparative compilation in SI Table 3), the results reflect several key points: 1) relatively high

625 belowground allocation; 2) low soil respiration in general, and low heterotrophic respiration in particular;  
626 3) combining the results for 2016 and those of our earlier study offered a long-term perspective across 13  
627 years, indicating that the low Rs in this ecosystem is robust and exhibits reduced sensitivity to temperature,  
628 and 4) there is a general long-term shift from autotrophic to heterotrophic respiration.

629 Comparing CO<sub>2</sub> fluxes in this forest with fluxes in a range of European forests showed that mean NEP in  
630 the semi-arid forest (167 g C m<sup>-2</sup> y<sup>-1</sup>) is similar to the mean NEP in other European forests (150 g C m<sup>-2</sup> y<sup>-1</sup>;  
631 FLUXNET).

632 Carbon partitioning belowground (TBCA/GPP) was relatively high (~38%), with little change across the  
633 long-term observation period. It is, however, within the range of mean value for forests in different biomes  
634 (Litton et al., 2007). High belowground allocation helps explain the high rate of SOC accumulation  
635 observed over the period since afforestation (Grünzweig et al., 2007; Qubaja et al., in press). Note that,  
636 irrespective of the soil carbon accumulation, the abiotic component to the CO<sub>2</sub> flux seems to be significant  
637 in dry environments (Table 3) and in particular in the dry seasons, when biological activities drastically  
638 decrease (Kowalski et al., 2008; Lopez-Ballesteros et al., 2017; Serrano-Ortiz et al., 2010; Martí-Roura et  
639 al., 2019). The results show that considering the abiotic effects on estimating soil respiration and, in turn,  
640 on estimating the carbon budget in dry calcareous soils can play an important part in estimating soil and  
641 ecosystem respiration fluxes (Angert et al., 2015; Roland et al., 2012).

642 The soil CO<sub>2</sub> efflux in the semi-arid forest (295 g C m<sup>-2</sup> y<sup>-1</sup>) is at the low end of Rs values across the range  
643 of climatic regions, from 50 to 2,750 g C m<sup>-2</sup> y<sup>-1</sup> (Adachi et al., 2017; Chen et al., 2014; Grünzweig et al.,  
644 2009; Hashimoto et al., 2015). This is clearly lower than the mean Rs value for global evergreen needle  
645 forests, which is estimated at 690 g C m<sup>-2</sup> y<sup>-1</sup> (Chen et al., 2014), and between estimates for desert scrub  
646 and Mediterranean woodland (224–713 g C m<sup>-2</sup> y<sup>-1</sup>; Raich and Schlesinger, 1992) or for Mediterranean  
647 forests (561–1,015 g C m<sup>-2</sup> y<sup>-1</sup>; Casals et al., 2011; Luysaert et al., 2007; Matteucci et al., 2015; Misson et  
648 al., 2010; Rey et al., 2002; Rodeghiero and Cescatti, 2005). The mean instantaneous rate of Rs, 0.8 μmol  
649 m<sup>-2</sup> s<sup>-1</sup>, is also in the range reported for unmanaged forest and grassland in the dry Mediterranean region  
650 (0.5 and 2.1 μmol m<sup>-2</sup> s<sup>-1</sup>; Correia et al., 2012).

651 The observed low Rs values were associated with a relatively high fraction of autotrophic and a lower  
652 fraction of heterotrophic respiration. The mean annual-scale R<sub>sa</sub>/R<sub>s</sub> ratio of 0.40 was at the high end of the  
653 global range of 0.09 to 0.49 (Chen et al., 2014; Hashimoto et al., 2015). In contrast, heterotrophic  
654 respiration showed an annual-scale R<sub>h</sub>/R<sub>s</sub> ratio of 0.39 ± 0.02 (Table 2 and Fig. 3), which is lower than the  
655 estimated global mean R<sub>h</sub>/R<sub>s</sub> value of 0.56 (Hashimoto et al., 2015), but within the range of Mediterranean  
656 region forest, which varies between 0.29 to 0.77 (Casals et al., 2011; Luysaert et al., 2007; Matteucci et

657 al., 2015; Misson et al., 2010; Rey et al., 2002; Rodeghiero and Cescatti, 2005). The relatively low annual  
658 scale of the heterotrophic respiration to  $R_s$  is consistent with the dry soil over much of the year in this  
659 forest (Fig 2 and SI Fig. 6) and the observed low decomposability of plant detritus and high mean SOC  
660 accumulation rate (Grünzweig et al., 2007).

661 The long-term perspective from the 13-year observation period indicates emerging trends that can be a  
662 basis for assessing the effects of forest age and the ~~marked~~evident increase in LAI (Table 3) and changes  
663 in environmental conditions (generally warming and drying; see, e.g., Lelieveld et al., 2012). ~~As noted~~  
664 ~~above,~~Here, because comparing the non-continuous data from the present (2016) and earlier (2001–2006)  
665 studies is sensitive to the large interannual variations in the ecosystem activities and fluxes (Qubaja et al.,  
666 in press), ~~and we therefore~~ focused on the more robust changes in the ratio of the respiration components  
667 to the overall fluxes ( $R_e$ ) (Table 3). This shows a shifting trend from the autotrophic components to the  
668 heterotrophic, with little change in the contribution of  $R_s$  to the overall efflux. The ratios of  $R_{sa}$ ,  $R_l$ , and  
669  $R_w$  to  $R_e$  tended to decrease by about 13%, while that of  $R_h$  increased by about 18%; similar trends were  
670 seen in soil respiration, with  $R_{sa}/R_s$  decreasing by -19% and  $R_h/R_s$  increasing by +8% (Table 3). The  
671 relatively low  $R_s$  under conditions of high temperature in the semi-arid ecosystem implies reduced  
672 sensitivity of respiration to temperature. This is partly imposed by low SWC conditions during extended  
673 parts of the year (Grünzweig et al., 2009; cf. Rey et al., 2002; Xu and Qi, 2001). Accordingly,  $R_s$  showed  
674 greater sensitivity to  $T_s$  in the wet period, but during the 8–9 months of the year when SWC was below  
675  $\sim 0.2 \text{ m}^3 \text{ m}^{-3}$ ,  $R_s$  varied predominantly with water availability. The long-term perspective reported in Table  
676 3 indicates a further decrease in temperature sensitivity, with mean  $Q_{10}$  values in the dry season decreasing  
677 from 1.6 to 1.1. These estimated  $Q_{10}$  values are generally consistent with published values for different  
678 ecosystems (1.4 to 2.0; Hashimoto et al., 2015; Zhou et al., 2009) and with low values under low SWC  
679 (Reichstein et al., 2003; Tang et al., 2005). This is also consistent with soil warming experiments by  $0.76^\circ\text{C}$   
680 in Mediterranean ecosystems, which decreased the  $R_s$  by 16%, and  $Q_{10}$  by 14% (Wang et al., 2014). Note  
681 also that the low temperature sensitivity in the dry season is likely to be related to reduced microbial  
682 activity, but may also involve downregulation of plant activity (Maseyk et al., 2008a) and drought-induced  
683 dormancy of shallow roots (Schiller, 2000). Finally, we also note that the greater importance of moisture  
684 availability in influencing respiration is clearly apparent from the observed relationships of  $R_s$  and  $R_h$  to  
685 mean annual precipitation (MAP) in European evergreen needle forests (SI Fig. 8; see also Grünzweig et  
686 al., 2007), which are not observed with respect to mean annual temperature.

### 687 *Data availability*

688 The data used in this study are archived and available from the corresponding author upon request  
689 ([dan.yakir@weizmann.ac.il](mailto:dan.yakir@weizmann.ac.il)).



690 ***Author contributions***

691 RQ and DY designed the study; RQ, FT, ER and DY performed the experiments. RQ and DY analyzed the  
692 data. DY and RQ wrote the paper, with discussions and contributions to interpretations of the results from  
693 all co-authors.

694 ***Competing interests***

695 The authors declare that they have no conflict of interest.

696 **5. Acknowledgements**

697 This long-term study was funded by the Forestry Department of Keren-Kayemeth-LeIsrael (KKL) and the  
698 German Research Foundation (DFG) as part of the project “Climate feedback and benefits of semi-arid  
699 forests” (CliFF) and by the Israel Ministry of Science and the Ministry of National Education, Higher  
700 Education, and Research (MENESR) of France (IMOS-French Program: 3-6735). The authors thank Efrat  
701 Schwartz for assistance with lab work. The long-term operation of the Yatir Forest Research Field Site is  
702 supported by the Cathy Wills and Robert Lewis Program in Environmental Science. We thank the entire  
703 Yatir team for technical support and the local KKL personnel for their cooperation.

704 **6. References**

- 705  
706 Adachi, M., Ito, A., Yonemura, S., and Takeuchi, W.: Estimation of global soil respiration by accounting for land-  
707 use changes derived from remote sensing data, *Journal of Environmental Management*, 200, 97-104,  
708 10.1016/j.jenvman.2017.05.076, 2017.
- 709 Angert, A., Yakir, D., Rodeghiero, M., Preisler, Y., Davidson, E. A., and Weiner, T.: Using O-2 to study the  
710 relationships between soil CO<sub>2</sub> efflux and soil respiration, *Biogeosciences*, 12, 2089-2099, 10.5194/bg-12-2089-  
711 2015, 2015.
- 712 Aubinet, M., Grelle, A., Ibrom, A., Rannik, U., Moncrieff, J., Foken, T., Kowalski, A. S., Martin, P. H., Berbigier,  
713 P., Bernhofer, C., Clement, R., Elbers, J., Granier, A., Grunwald, T., Morgenstern, K., Pilegaard, K., Rebmann,  
714 C., Snijders, W., Valentini, R., and Vesala, T.: Estimates of the annual net carbon and water exchange of forests:  
715 The EUROFLUX methodology, *Advances in Ecological Research*, Vol 30, 30, 113-175, 2000.
- 716 Bahn, M., Janssens, I. A., Reichstein, M., Smith, P., and Trumbore, S. E.: Soil respiration across scales: towards an  
717 integration of patterns and processes, *New Phytologist*, 186, 292-296, 10.1111/j.1469-8137.2010.03237.x, 2010.
- 718 Balogh, J., Pinter, K., Foti, S., Cserhalmi, D., Papp, M., and Nagy, Z.: Dependence of soil respiration on soil moisture,  
719 clay content, soil organic matter, and CO<sub>2</sub> uptake in dry grasslands, *Soil Biology & Biochemistry*, 43, 1006-  
720 1013, 10.1016/j.soilbio.2011.01.017, 2011.
- 721 Binkley, D., Stape, J. L., Takahashi, E. N., and Ryan, M. G.: Tree-girdling to separate root and heterotrophic  
722 respiration in two Eucalyptus stands in Brazil, *Oecologia*, 148, 447-454, 10.1007/s00442-006-0383-6, 2006.
- 723 Bonan, G. B.: *Ecological climatology : concepts and applications*, 2nd ed., ed., Cambridge : Cambridge University  
724 Press, Cambridge, 2008.
- 725 Bond-Lamberty, B., and Thomson, A.: Temperature-associated increases in the global soil respiration record, *Nature*,  
726 464, 579-U132, 10.1038/nature08930, 2010.
- 727 Buchmann, N.: Biotic and abiotic factors controlling soil respiration rates in *Picea abies* stands, *Soil Biology &*

728 Biochemistry, 32, 1625-1635, 10.1016/s0038-0717(00)00077-8, 2000.

729 Carbone, M. S., Winston, G. C., and Trumbore, S. E.: Soil respiration in perennial grass and shrub ecosystems:  
730 Linking environmental controls with plant and microbial sources on seasonal and diel timescales, *Journal of*  
731 *Geophysical Research-Biogeosciences*, 113, 10.1029/2007jg000611, 2008.

732 Carmi, I., Yakir, D., Yechieli, Y., Kronfeld, J., and Stiller, M.: VARIATIONS IN SOIL CO<sub>2</sub> CONCENTRATIONS  
733 AND ISOTOPIC VALUES IN A SEMI-ARID REGION DUE TO BIOTIC AND ABIOTIC PROCESSES IN  
734 THE UNSATURATED ZONE, *Radiocarbon*, 55, 932-942, 2013.

735 Carvalhais, N., Forkel, M., Khomik, M., Bellarby, J., Jung, M., Migliavacca, M., Mu, M. Q., Saatchi, S., Santoro,  
736 M., Thurner, M., Weber, U., Ahrens, B., Beer, C., Cescatti, A., Randerson, J. T., and Reichstein, M.: Global  
737 covariation of carbon turnover times with climate in terrestrial ecosystems, *Nature*, 514, 213-+,  
738 10.1038/nature13731, 2014.

739 Casals, P., Lopez-Sangil, L., Carrara, A., Gimeno, C., and Nogues, S.: Autotrophic and heterotrophic contributions  
740 to short-term soil CO<sub>2</sub> efflux following simulated summer precipitation pulses in a Mediterranean dehesa, *Global*  
741 *Biogeochemical Cycles*, 25, 10.1029/2010gb003973, 2011.

742 Chen, D., Zhang, Y., Lin, Y., Zhu, W., and Fu, S.: Changes in belowground carbon in *Acacia crassicarpa* and  
743 *Eucalyptus urophylla* plantations after tree girdling, *Plant and Soil*, 326, 123-135, 10.1007/s11104-009-9986-0,  
744 2010.

745 Chen, S. T., Zou, J. W., Hu, Z. H., Chen, H. S., and Lu, Y. Y.: Global annual soil respiration in relation to climate,  
746 soil properties and vegetation characteristics: Summary of available data, *Agricultural and Forest Meteorology*,  
747 198, 335-346, 10.1016/j.agrformet.2014.08.020, 2014.

748 Conant, R. T., Klopatek, J. M., Malin, R. C., and Klopatek, C. C.: Carbon pools and fluxes along an environmental  
749 gradient in northern Arizona, *Biogeochemistry*, 43, 43-61, 10.1023/a:1006004110637, 1998.

750 Correia, A. C., Minunno, F., Caldeira, M. C., Banza, J., Mateus, J., Carneiro, M., Wingate, L., Shvaleyeva, A., Ramos,  
751 A., Jongen, M., Bugalho, M. N., Nogueira, C., Lecomte, X., and Pereira, J. S.: Soil water availability strongly  
752 modulates soil CO<sub>2</sub> efflux in different Mediterranean ecosystems: Model calibration using the Bayesian  
753 approach, *Agriculture Ecosystems & Environment*, 161, 88-100, 10.1016/j.agee.2012.07.025, 2012.

754 Davidson, E. A., and Janssens, I. A.: Temperature sensitivity of soil carbon decomposition and feedbacks to climate  
755 change, *Nature*, 440, 165-173, 10.1038/nature04514, 2006.

756 DeLucia, E. H., Drake, J. E., Thomas, R. B., and Gonzalez-Meler, M.: Forest carbon use efficiency: is respiration a  
757 constant fraction of gross primary production?, *Global Change Biology*, 13, 1157-1167, 10.1111/j.1365-  
758 2486.2007.01365.x, 2007.

759 Deng, Q., Hui, D., Zhang, D., Zhou, G., Liu, J., Liu, S., Chu, G., and Li, J.: Effects of Precipitation Increase on Soil  
760 Respiration: A Three-Year Field Experiment in Subtropical Forests in China, *Plos One*, 7,  
761 10.1371/journal.pone.0041493, 2012.

762 Etzold, S., Ruehr, N. K., Zweifel, R., Dobbertin, M., Zingg, A., Pluess, P., Hasler, R., Eugster, W., and Buchmann,  
763 N.: The Carbon Balance of Two Contrasting Mountain Forest Ecosystems in Switzerland: Similar Annual  
764 Trends, but Seasonal Differences, *Ecosystems*, 14, 1289-1309, 10.1007/s10021-011-9481-3, 2011.

765 Etzold, S., Zweifel, R., Ruehr, N. K., Eugster, W., and Buchmann, N.: Long-term stem CO<sub>2</sub> concentration  
766 measurements in Norway spruce in relation to biotic and abiotic factors, *New Phytologist*, 197, 1173-1184,  
767 10.1111/nph.12115, 2013.

768 Falge, E., Baldocchi, D., Tenhunen, J., Aubinet, M., Bakwin, P., Berbigier, P., Bernhofer, C., Burba, G., Clement,  
769 R., Davis, K. J., Elbers, J. A., Goldstein, A. H., Grelle, A., Granier, A., Guomundsson, J., Hollinger, D.,  
770 Kowalski, A. S., Katul, G., Law, B. E., Malhi, Y., Meyers, T., Monson, R. K., Munger, J. W., Oechel, W., Paw,  
771 K. T., Pilegaard, K., Rannik, U., Rebmann, C., Suyker, A., Valentini, R., Wilson, K., and Wofsy, S.: Seasonality  
772 of ecosystem respiration and gross primary production as derived from FLUXNET measurements, *Agricultural*  
773 *and Forest Meteorology*, 113, 53-74, 10.1016/s0168-1923(02)00102-8, 2002.

774 Flechard, C. R., Ibrom, A., Skiba, U. M., de Vries, W., van Oijen, M., Cameron, D. R., Dise, N. B., Korhonen, J. F.  
775 J., Buchmann, N., Legout, A., Simpson, D., Sanz, M. J., Aubinet, M., Loustau, D., Montagnani, L., Neiryneck, J.,  
776 Janssens, I. A., Pihlatie, M., Kiese, R., Siemens, J., Francez, A.-J., Augustin, J., Varlagin, A., Olejnik, J.,  
777 Juszczak, R., Aurela, M., Chojnicki, B. H., Dämmgen, U., Djuricic, V., Drewer, J., Eugster, W., Fauvel, Y.,  
778 Fowler, D., Frumau, A., Granier, A., Gross, P., Hamon, Y., Helfter, C., Hensen, A., Horváth, L., Kitzler, B.,  
779 Kruijt, B., Kutsch, W. L., Lobo-do-Vale, R., Lohila, A., Longdoz, B., Marek, M. V., Matteucci, G., Mitosinkova,  
780 M., Moreaux, V., Neftel, A., Ourcival, J.-M., Pilegaard, K., Pita, G., Sanz, F., Schjoerring, J. K., Sebastia, M.-  
781 T., Tang, Y. S., Uggerud, H., Urbaniak, M., van Dijk, N., Vesala, T., Vidic, S., Vincke, C., Weidinger, T.,  
782 Zechmeister-Boltenstern, S., Butterbach-Bahl, K., Nemitz, E., and Sutton, M. A.: Carbon / nitrogen interactions  
783 in European forests and semi-natural vegetation. Part I: Fluxes and budgets of carbon, nitrogen and greenhouse  
784 gases from ecosystem monitoring and modelling, *Biogeosciences Discuss.*, <https://doi.org/10.5194/bg-2019-333>,

785 in review, 2019a.

786 Flechard, C. R., van Oijen, M., Cameron, D. R., de Vries, W., Ibrom, A., Buchmann, N., Dise, N. B., Janssens, I. A.,  
787 Neiryneck, J., Montagnani, L., Varlagin, A., Loustau, D., Legout, A., Ziemblińska, K., Aubinet, M., Aurela, M.,  
788 Chojnicki, B. H., Drewer, J., Eugster, W., Francez, A.-J., Juszczak, R., Kitzler, B., Kutsch, W. L., Lohila, A.,  
789 Longdoz, B., Matteucci, G., Moreaux, V., Neftel, A., Olejnik, J., Sanz, M. J., Siemens, J., Vesala, T., Vincke,  
790 C., Nemitz, E., Zechmeister-Boltenstern, S., Butterbach-Bahl, K., Skiba, U. M., and Sutton, M. A.:  
791 Carbon / nitrogen interactions in European forests and semi-natural vegetation. Part II: Untangling climatic,  
792 edaphic, management and nitrogen deposition effects on carbon sequestration potentials, *Biogeosciences*  
793 Discuss., <https://doi.org/10.5194/bg-2019-335>, in review, 2019b.

794 Frank, A. B., Liebig, M. A., and Hanson, J. D.: Soil carbon dioxide fluxes in northern semiarid grasslands, *Soil*  
795 *Biology & Biochemistry*, 34, 1235-1241, 10.1016/s0038-0717(02)00062-7, 2002.

796 Frey, B., Hagedorn, F., and Giudici, F.: Effect of girdling on soil respiration and root composition in a sweet chestnut  
797 forest, *Forest Ecology and Management*, 225, 271-277, 10.1016/j.foreco.2006.01.003, 2006.

798 Gelfand, I., Grünzweig, J. M., and Yakir, D.: Slowing of nitrogen cycling and increasing nitrogen use efficiency  
799 following afforestation of semi-arid shrubland, *Oecologia*, 168, 563-575, 10.1007/s00442-011-2111-0, 2012.

800 Giardina, C. P., and Ryan, M. G.: Total belowground carbon allocation in a fast-growing Eucalyptus plantation  
801 estimated using a carbon balance approach, *Ecosystems*, 5, 487-499, 10.1007/s10021-002-0130-8, 2002.

802 Graven, H. D., Guilderson, T. P., and Keeling, R. F.: Observations of radiocarbon in CO<sub>2</sub> at La Jolla, California,  
803 USA 1992-2007: Analysis of the long-term trend, *Journal of Geophysical Research-Atmospheres*, 117,  
804 10.1029/2011jd016533, 2012.

805 Grünzweig, J. M., Gelfand, I., Fried, Y., and Yakir, D.: Biogeochemical factors contributing to enhanced carbon  
806 storage following afforestation of a semi-arid shrubland, *Biogeosciences*, 4, 891-904, 2007.

807 Grünzweig, J. M., Hemming, D., Maseyk, K., Lin, T., Rotenberg, E., Raz-Yaseef, N., Falloon, P. D., and Yakir, D.:  
808 Water limitation to soil CO<sub>2</sub> efflux in a pine forest at the semiarid "timberline", *Journal of Geophysical Research-*  
809 *Biogeosciences*, 114, 10.1029/2008jg000874, 2009.

810 Grünzweig, J. M., Lin, T., Rotenberg, E., Schwartz, A., and Yakir, D.: Carbon sequestration in arid-land forest,  
811 *Global Change Biology*, 9, 791-799, 10.1046/j.1365-2486.2003.00612.x, 2003.

812 Hagedorn, F., Joseph, J., Peter, M., Luster, J., Pritsch, K., Geppert, U., Kerner, R., Molinier, V., Egli, S., Schaub, M.,  
813 Liu, J. F., Li, M. H., Sever, K., Weiler, M., Siegwolf, R. T. W., Gessler, A., and Arend, M.: Recovery of trees  
814 from drought depends on belowground sink control, *Nature Plants*, 2, 10.1038/nplants.2016.111, 2016.

815 Hashimoto, S., Carvalhais, N., Ito, A., Migliavacca, M., Nishina, K., and Reichstein, M.: Global spatiotemporal  
816 distribution of soil respiration modeled using a global database, *Biogeosciences*, 12, 4121-4132, 10.5194/bg-12-  
817 4121-2015, 2015.

818 Hemming, D., Yakir, D., Ambus, P., Aurela, M., Besson, C., Black, K., Buchmann, N., Burlett, R., Cescatti, A.,  
819 Clement, R., Gross, P., Granier, A., Grunwald, T., Havrankova, K., Janous, D., Janssens, I. A., Knohl, A., Ostner,  
820 B. K., Kowalski, A., Laurila, T., Mata, C., Marcolla, B., Matteucci, G., Moncrieff, J., Moors, E. J., Osborne, B.,  
821 Pereira, J. S., Pihlatie, M., Pilegaard, K., Ponti, F., Rosova, Z., Rossi, F., Scartazza, A., and Vesala, T.: Pan-  
822 European delta C-13 values of air and organic matter from forest ecosystems, *Global Change Biology*, 11, 1065-  
823 1093, 10.1111/j.1365-2486.2005.00971.x, 2005.

824 Hogberg, P., Bhupinderpal, S., Lofvenius, M. O., and Nordgren, A.: Partitioning of soil respiration into its autotrophic  
825 and heterotrophic components by means of tree-girdling in old boreal spruce forest, *Forest Ecology and*  
826 *Management*, 257, 1764-1767, 10.1016/j.foreco.2009.01.036, 2009.

827 Hui, D. F., and Luo, Y. Q.: Evaluation of soil CO<sub>2</sub> production and transport in Duke Forest using a process-based  
828 modeling approach, *Global Biogeochemical Cycles*, 18, 10.1029/2004gb002297, 2004.

829 IPCC. Climate Change 2014: Mitigation of Climate Change. Contribution of Working Group III to the Fifth  
830 Assessment Report of the Intergovernmental Panel on Climate Change [Edenhofer, O., R. et al.]. Cambridge  
831 University Press, Cambridge and New York, 2014.

832 Jiang, H., Deng, Q., Zhou, G., Hui, D., Zhang, D., Liu, S., Chu, G., and Li, J.: Responses of soil respiration and its  
833 temperature/moisture sensitivity to precipitation in three subtropical forests in southern China, *Biogeosciences*,  
834 10, 3963-3982, 10.5194/bg-10-3963-2013, 2013.

835 Joseph, J., Kulls, C., Arend, M., Schaub, M., Hagedorn, F., Gessler, A., and Weiler, M.: Application of a laser-based  
836 spectrometer for continuous in situ measurements of stable isotopes of soil CO<sub>2</sub> in calcareous and acidic soils,  
837 *Soil*, 5, 49-62, 10.5194/soil-5-49-2019, 2019.

838 Kool, D. M., Chung, H. G., Tate, K. R., Ross, D. J., Newton, P. C. D., and Six, J.: Hierarchical saturation of soil  
839 carbon pools near a natural CO<sub>2</sub> spring, *Global Change Biology*, 13, 1282-1293, 10.1111/j.1365-  
840 2486.2007.01362.x, 2007.

841 Kowalski, A. S., Serrano-Ortiz, P., Janssens, I. A., Sanchez-Moral, S., Cuezva, S., Domingo, F., Were, A., and

- 842 Alados-Arboledas, L.: Can flux tower research neglect geochemical CO<sub>2</sub> exchange?, *Agricultural and Forest*  
843 *Meteorology*, 148, 1045-1054, 10.1016/j.agrformet.2008.02.004, 2008.
- 844 Kuzyakov, Y.: Sources of CO<sub>2</sub> efflux from soil and review of partitioning methods, *Soil Biology & Biochemistry*,  
845 38, 425-448, 10.1016/j.soilbio.2005.08.020, 2006.
- 846 Lelieveld, J., Hadjinicolaou, P., Kostopoulou, E., Chenoweth, J., El Maayar, M., Giannakopoulos, C., Hannides, C.,  
847 Lange, M. A., Tanarhte, M., Tyrllis, E., and Xoplaki, E.: Climate change and impacts in the Eastern Mediterranean  
848 and the Middle East, *Climatic Change*, 114, 667-687, 10.1007/s10584-012-0418-4, 2012.
- 849 Lellei-Kovacs, E., Kovacs-Lang, E., Botta-Dukat, Z., Kalapos, T., Emmett, B., and Beier, C.: Thresholds and  
850 interactive effects of soil moisture on the temperature response of soil respiration, *European Journal of Soil*  
851 *Biology*, 47, 247-255, 10.1016/j.ejsobi.2011.05.004, 2011.
- 852 Levin, I., Naegler, T., Kromer, B., Diehl, M., Francey, R. J., Gomez-Pelaez, A. J., Steele, L. P., Wagenbach, D.,  
853 Weller, R., and Worthy, D. E.: Observations and modelling of the global distribution and long-term trend of  
854 atmospheric (CO<sub>2</sub>)-C-14 (vol 62, pg 26, 2010), *Tellus Series B-Chemical and Physical Meteorology*, 62, 207-  
855 207, 10.1111/j.1600-0889.2010.00456.x, 2010.
- 856 Lin, G. H., Ehleringer, J. R., Rygielwicz, P. T., Johnson, M. G., and Tingey, D. T.: Elevated CO<sub>2</sub> and temperature  
857 impacts on different components of soil CO<sub>2</sub> efflux in Douglas-fir terracosms, *Global Change Biology*, 5, 157-  
858 168, 10.1046/j.1365-2486.1999.00211.x, 1999.
- 859 Litton, C. M., Raich, J. W., and Ryan, M. G.: Carbon allocation in forest ecosystems, *Global Change Biology*, 13,  
860 2089-2109, 10.1111/j.1365-2486.2007.01420.x, 2007.
- 861 Lopez-Ballesteros, A., Serrano-Ortiz, P., Kowalski, A. S., Sanchez-Canete, E. P., Scott, R. L., and Domingo, F.:  
862 Subterranean ventilation of allochthonous CO<sub>2</sub> governs net CO<sub>2</sub> exchange in a semiarid Mediterranean  
863 grassland, *Agricultural and Forest Meteorology*, 234, 115-126, 10.1016/j.agrformet.2016.12.021, 2017.
- 864 Luyssaert, S., Inglima, I., Jung, M., Richardson, A. D., Reichstein, M., Papale, D., Piao, S. L., Schulzes, E. D.,  
865 Wingate, L., Matteucci, G., Aragao, L., Aubinet, M., Beers, C., Bernhofer, C., Black, K. G., Bonal, D.,  
866 Bonnefond, J. M., Chambers, J., Ciais, P., Cook, B., Davis, K. J., Dolman, A. J., Gielen, B., Goulden, M., Grace,  
867 J., Granier, A., Grelle, A., Griffis, T., Grunwald, T., Guidolotti, G., Hanson, P. J., Harding, R., Hollinger, D. Y.,  
868 Hutyrá, L. R., Kolar, P., Kruijt, B., Kutsch, W., Lagergren, F., Laurila, T., Law, B. E., Le Maire, G., Lindroth,  
869 A., Loustau, D., Malhi, Y., Mateus, J., Migliavacca, M., Misson, L., Montagnani, L., Moncrieff, J., Moors, E.,  
870 Munger, J. W., Nikinmaa, E., Ollinger, S. V., Pita, G., Rebmann, C., Rouspard, O., Saigusa, N., Sanz, M. J.,  
871 Seufert, G., Sierra, C., Smith, M. L., Tang, J., Valentini, R., Vesala, T., and Janssens, I. A.: CO<sub>2</sub> balance of  
872 boreal, temperate, and tropical forests derived from a global database, *Global Change Biology*, 13, 2509-2537,  
873 10.1111/j.1365-2486.2007.01439.x, 2007.
- 874 Maseyk, K., Grünzweig, J. M., Rotenberg, E., and Yakir, D.: Respiration acclimation contributes to high carbon-use  
875 efficiency in a seasonally dry pine forest, *Global Change Biology*, 14, 1553-1567, 10.1111/j.1365-  
876 2486.2008.01604.x, 2008a.
- 877 Matteucci, M., Gruening, C., Ballarin, I. G., Seufert, G., and Cescatti, A.: Components, drivers and temporal  
878 dynamics of ecosystem respiration in a Mediterranean pine forest, *Soil Biology & Biochemistry*, 88, 224-235,  
879 10.1016/j.soilbio.2015.05.017, 2015.
- 880 Misson, L., Rocheteau, A., Rambal, S., Ourcival, J. M., Limousin, J. M., and Rodriguez, R.: Functional changes in  
881 the control of carbon fluxes after 3 years of increased drought in a Mediterranean evergreen forest?, *Global*  
882 *Change Biology*, 16, 2461-2475, 10.1111/j.1365-2486.2009.02121.x, 2010.
- 883 Pataki, D. E., Ehleringer, J. R., Flanagan, L. B., Yakir, D., Bowling, D. R., Still, C. J., Buchmann, N., Kaplan, J. O.,  
884 and Berry, J. A.: The application and interpretation of Keeling plots in terrestrial carbon cycle research, *Global*  
885 *Biogeochemical Cycles*, 17, 10.1029/2001gb001850, 2003.
- 886 Peterjohn, W. T., Melillo, J. M., Steudler, P. A., Newkirk, K. M., Bowles, F. P., and Aber, J. D.: RESPONSES OF  
887 TRACE GAS FLUXES AND N AVAILABILITY TO EXPERIMENTALLY ELEVATED SOIL  
888 TEMPERATURES, *Ecological Applications*, 4, 617-625, 10.2307/1941962, 1994.
- 889 Poulter, B., Frank, D., Ciais, P., Myneni, R. B., Andela, N., Bi, J., Broquet, G., Canadell, J. G., Chevallier, F., Liu,  
890 Y. Y., Running, S. W., Sitch, S., and van der Werf, G. R.: Contribution of semi-arid ecosystems to interannual  
891 variability of the global carbon cycle, *Nature*, 509, 600-+, 10.1038/nature13376, 2014.
- 892 Preisler, Y., Tatarinov, F., Grunzweig, J. M., Bert, D., Ogee, J., Wingate, L., Rotenberg, E., Rohatyn, S., Her, N.,  
893 Moshe, I., Klein, T., and Yakir, D.: Mortality versus survival in drought-affected Aleppo pine forest depends on  
894 the extent of rock cover and soil stoniness, *Functional Ecology*, 33, 901-912, 10.1111/1365-2435.13302, 2019.
- 895 Qubaja, R., Grünzweig, J., Rotenberg, E., and Yakir, D.: Evidence for large carbon sink and long residence time in  
896 semiarid forests based on 15 year flux and inventory records. *Global Change Biology*, 10.1111/gcb.14927, 2019.
- 897 Raich, J. W., and Schlesinger, W. H.: THE GLOBAL CARBON-DIOXIDE FLUX IN SOIL RESPIRATION AND  
898 ITS RELATIONSHIP TO VEGETATION AND CLIMATE, *Tellus Series B-Chemical and Physical*

- 899 Meteorology, 44, 81-99, 10.1034/j.1600-0889.1992.t01-1-00001.x, 1992.
- 900 Ramnarine, R., Wagner-Riddle, C., Dunfield, K. E., and Voroney, R. P.: Contributions of carbonates to soil CO<sub>2</sub>
- 901 emissions, Canadian Journal of Soil Science, 92, 599-607, 10.4141/cjss2011-025, 2012.
- 902 Raz-Yaseef, N., Rotenberg, E., and Yakir, D.: Effects of spatial variations in soil evaporation caused by tree shading
- 903 on water flux partitioning in a semi-arid pine forest, Agricultural and Forest Meteorology, 150, 454-462,
- 904 10.1016/j.agrformet.2010.01.010, 2010.
- 905 Reichstein, M., Rey, A., Freibauer, A., Tenhunen, J., Valentini, R., Banza, J., Casals, P., Cheng, Y. F., Grünzweig,
- 906 J. M., Irvine, J., Joffre, R., Law, B. E., Loustau, D., Miglietta, F., Oechel, W., Ourcival, J. M., Pereira, J. S.,
- 907 Peressotti, A., Ponti, F., Qi, Y., Rambal, S., Rayment, M., Romanya, J., Rossi, F., Tedeschi, V., Tirone, G., Xu,
- 908 M., and Yakir, D.: Modeling temporal and large-scale spatial variability of soil respiration from soil water
- 909 availability, temperature and vegetation productivity indices, Global Biogeochemical Cycles, 17,
- 910 10.1029/2003gb002035, 2003.
- 911 Rey, A., Pegoraro, E., Tedeschi, V., De Parri, I., Jarvis, P. G., and Valentini, R.: Annual variation in soil respiration
- 912 and its components in a coppice oak forest in Central Italy, Global Change Biology, 8, 851-866, 10.1046/j.1365-
- 913 2486.2002.00521.x, 2002.
- 914 Rodeghiero, M., and Cescatti, A.: Main determinants of forest soil respiration along an elevation/temperature gradient
- 915 in the Italian Alps, Global Change Biology, 11, 1024-1041, 10.1111/j.1365-2486.2005.00963.x, 2005.
- 916 Roland, M.: Contributions of carbonate weathering to the net ecosystem carbon balance of a mediterranean forest,
- 917 Ph.D. thesis, Antwerpen University, Antwerpen, Belgium, 2012.
- 918 Ross, I., Misson, L., Rambal, S., Arneth, A., Scott, R. L., Carrara, A., Cescatti, A., and Genesio, L.: How do variations
- 919 in the temporal distribution of rainfall events affect ecosystem fluxes in seasonally water-limited Northern
- 920 Hemisphere shrublands and forests?, Biogeosciences, 9, 1007-1024, 10.5194/bg-9-1007-2012, 2012.
- 921 Rotenberg, E., and Yakir, D.: Contribution of Semi-Arid Forests to the Climate System, Science, 327, 451-454,
- 922 10.1126/science.1179998, 2010.
- 923 Schiller, G.: Ecophysiology of *Pinus halepensis* Mill. and *P. brutia* Ten, in Ecology, Biogeography and Management
- 924 of *Pinus halepensis* and *P. brutia* Forest Ecosystems in the Mediterranean Basin, edited by: Ne'eman, G., and
- 925 Trabaud, L., Backhuys, Leiden, Netherlands, 51-65, 2000.
- 926 Serrano-Ortiz, P., Roland, M., Sanchez-Moral, S., Janssens, I. A., Domingo, F., Godderis, Y., and Kowalski, A. S.:
- 927 Hidden, abiotic CO<sub>2</sub> flows and gaseous reservoirs in the terrestrial carbon cycle: Review and perspectives,
- 928 Agricultural and Forest Meteorology, 150, 321-329, 10.1016/j.agrformet.2010.01.002, 2010.
- 929 Shachnovich, Y., Berliner, P. R., and Bar, P.: Rainfall interception and spatial distribution of throughfall in a pine
- 930 forest planted in an arid zone, Journal of Hydrology, 349, 168-177, 10.1016/j.jhydrol.2007.10.051, 2008.
- 931 Shen, W. J., Jenerette, G. D., Hui, D. F., Phillips, R. P., and Ren, H.: Effects of changing precipitation regimes on
- 932 dryland soil respiration and C pool dynamics at rainfall event, seasonal and interannual scales, Journal of
- 933 Geophysical Research-Biogeosciences, 113, 10.1029/2008jg000685, 2008.
- 934 Subke, J.-A., Voke, N. R., Leronni, V., Garnett, M. H., and Ineson, P.: Dynamics and pathways of autotrophic and
- 935 heterotrophic soil CO<sub>2</sub> efflux revealed by forest girdling, Journal of Ecology, 99, 186-193, 10.1111/j.1365-
- 936 2745.2010.01740.x, 2011.
- 937 Taneva, L., and Gonzalez-Meler, M. A.: Distinct patterns in the diurnal and seasonal variability in four components
- 938 of soil respiration in a temperate forest under free-air CO<sub>2</sub> enrichment, Biogeosciences, 8, 3077-3092,
- 939 10.5194/bg-8-3077-2011, 2011.
- 940 Tang, J. W., Baldocchi, D. D., and Xu, L.: Tree photosynthesis modulates soil respiration on a diurnal time scale,
- 941 Global Change Biology, 11, 1298-1304, 10.1111/j.1365-2486.2005.00987.x, 2005.
- 942 Tatarinov, F., Rotenberg, E., Maseyk, K., Ogee, J., Klein, T., and Yakir, D.: Resilience to seasonal heat wave episodes
- 943 in a Mediterranean pine forest, New Phytologist, 210, 485-496, 10.1111/nph.13791, 2016.
- 944 Taylor, A. J., Lai, C. T., Hopkins, F. M., Wharton, S., Bible, K., Xu, X. M., Phillips, C., Bush, S., and Ehleringer, J.
- 945 R.: Radiocarbon-Based Partitioning of Soil Respiration in an Old-Growth Coniferous Forest, Ecosystems, 18,
- 946 459-470, 10.1007/s10021-014-9839-4, 2015.
- 947 Volcani, A., Karnieli, A., and Svoray, T.: The use of remote sensing and GIS for spatio-temporal analysis of the
- 948 physiological state of a semi-arid forest with respect to drought years, Forest Ecology and Management, 215,
- 949 239-250, 10.1016/j.foreco.2005.05.063, 2005.
- 950 Wang, X., Liu, L. L., Piao, S. L., Janssens, I. A., Tang, J. W., Liu, W. X., Chi, Y. G., Wang, J., and Xu, S.: Soil
- 951 respiration under climate warming: differential response of heterotrophic and autotrophic respiration, Global
- 952 Change Biology, 20, 3229-3237, 10.1111/gcb.12620, 2014b.
- 953 Xu, M., and Qi, Y.: Soil-surface CO<sub>2</sub> efflux and its spatial and temporal variations in a young ponderosa pine
- 954 plantation in northern California, Global Change Biology, 7, 667-677, 10.1046/j.1354-1013.2001.00435.x, 2001.
- 955 Xu, Z. F., Tang, S. S., Xiong, L., Yang, W. Q., Yin, H. J., Tu, L. H., Wu, F. Z., Chen, L. H., and Tan, B.: Temperature

956 sensitivity of soil respiration in China's forest ecosystems: Patterns and controls, *Applied Soil Ecology*, 93, 105-  
957 110, 10.1016/j.apsoil.2015.04.008, 2015.

958 Yu, S. Q., Chen, Y. Q., Zhao, J., Fu, S. L., Li, Z., Xia, H. P., and Zhou, L. X.: Temperature sensitivity of total soil  
959 respiration and its heterotrophic and autotrophic components in six vegetation types of subtropical China, *Science*  
960 *of the Total Environment*, 607, 160-167, 10.1016/j.scitotenv.2017.06.194, 2017a.

961 Zhou, T., Shi, P. J., Hui, D. F., and Luo, Y. Q.: Global pattern of temperature sensitivity of soil heterotrophic  
962 respiration (Q(10)) and its implications for carbon-climate feedback, *Journal of Geophysical Research-*  
963 *Biogeosciences*, 114, 10.1029/2008jg000850, 2009.